University of Alberta

Asialofetuin-coated PLGA Nanoparticles for Targeting Hepatocytes

By

Gagandeep Kharaud

A thesis submitted to the Faculty of Graduate Studies and Research in partial fulfillment

of the requirements for the degree of

Master of Science

Faculty of Pharmacy and Pharmaceutical Sciences

Edmonton, Alberta

©Gagandeep Kharaud

Fall 2010

Edmonton, Alberta

Examining Committee

Dr. Kamaljit Kaur, Faculty of Pharmacy and Pharmaceutical Sciences

Dr. Mavanur Suresh, Faculty of Pharmacy and Pharmaceutical Sciences

Dr. Afsaneh Lavasanifar, Faculty of Pharmacy and Pharmaceutical Sciences

Dr. Hasan Uludag, Chemical and Materials Engineering, Faculty of Engineering

DEDICATED TO

My loving parents, Narinder and Surinder, for their love and support. Without their support and encouragement, this degree would not have been fulfilled.

My loving Brother, Simran Kharaud, who has always being there for me for emotional support.

ABSTRACT

The purpose of this project was to formulate, modify and evaluate nanoparticles for targeting asialoglycoprotein receptor found in large numbers exclusively on hepatocyte surfaces. Our goal is to increase the efficacy, reduce the side effects and the cost of the hydrophilic drugs administered to cure diseases like hepatitis C virus. Selective drug delivery into targeted cells using nanoparticles is one effective approach to enhance activity and avoid systemic side effects. Here we describe our effort towards the development of specially engineered poly(D,L-lactic-co-glycolic acid) nanoparticles using double emulsion method and surface coat them with asialofetuin for targeted delivery into hepatocytes. Bovine Serum Albumin-coated nanoparticles were prepared as a negative control. Furthermore, covalently conjugated protein on nanoparticle was labeled with rhodamine and was used for cell-based studies. Results from these studies indicated that asialofetuin conjugated with nanoparticles showed enhanced and selective uptake by hepatocytes compared to nanoparticles conjugated with Bovine Serum Albumin.

ACKNOWLEDGEMENTS

TABLE OF CONTENTS

LIST OF TABLES

LIST OF FIGURES

LIST OF ABBREVIATIONS

° C	Degrees Centigrade
λ	Wave Length
µg	Micro gram
µL	Micro liter
AFM	Atomic force microscope
ASF	Asialofetuin
ASGP-R	Asialoglycoprotein Receptor
BCA	Bicinchoninic Acid
BSA	Bovine Serum Albumin
CO_2	Carbon dioxide
cDNA	Complementary Deoxyribonucleic acid
DESE	Double Emulsion Solvent Evaporation
DMAB	Didodecyldimethylammonium bromide
DMEM	Dulbecco's Modified Eagle's Medium
DMSO	Dimethyl Sulfoxide
DNA	Diribonucleic Acid
EA	Ethyl Acetate
ED	Emulsification Diffusion
Rhodamine	5(6)-Carboxy-X-rhodamine N-succinimidyl ester
EDC	1-Ethyl-3-(3-dimethylaminopropyl) carbodiimidehydro-chloride
FA	Fatty Acid
FBS	Fetal Bovine Serum
FDA	Food and Drug Administration
HCC	Hepatocellular Carcinoma
HCV	Hepatitis C Virus
Hep G2	Heptocellular Human Liver Carcinoma Cell Line
HIV	Human Immunodeficiency Virus

hr	Hour
IR	Insulin Resistance
KDa	KiloDalton
Mol Wt.	Molecular Weight
mg	Milligram
min	Minute
mL	Milliliter
mM	Millimolar
NHS	N-hydroxy-succinimide
NHS-ester	N-hydroxy-succinimidyl-ester
nm	Nanometer
NP	Nanoparticles
OD	Optical Density
PB	Phosphate Buffer
PBS	Phosphate Buffered Saline
PC	Propylene Carbonate
PEG	Polyethylene Glycol
PGA	Poly (lactic acid)
PLA	Poly (glycolic acid)
PLGA	Poly (D,L-lactic-co-glycolic acid)
PVA	Polyvinyl alcohol
RNA	Ribonucleic Acid
rpm	Rotations Per Minute
SEM	Scanning Electron Microscopy
Tc	Collapse Temperature
TEM	Transmission Electron Microscopy

CHAPTER 1. Introduction

1.1 Targeted Delivery of Nanoparticles

1.1.1 Overview of Carriers used for Drug Delivery

A number of formulations have been designed and reported over the last few decades to target specific tissues or cell types to monitor diseases at early development stages and/or making it possible to improve the therapeutic efficacy while reducing deleterious side effects of the drugs [1-2]. For diagnostic applications, highly specific targeting is desirable for non-invasive imaging technologies so that signals from non-specific uptake by surrounding tissues can be reduced or eliminated [3]. For therapeutic application, specific targeted delivery is essential in order to diminish detrimental effects on healthy tissue. For both diagnostic and therapeutic applications, it is also essential that upon administration the delivery characteristics stays constant and are not considerably altered by host defense mechanisms. Nano-objects such as micelles or liposomes can be used to target specific tissues or cells.

Micelle is formed when a variety of molecules including soaps and detergents are added to water [4]. Micelle is an aggregate of surfactant molecules dispersed in a liquid colloid. Polymeric micelles are composed of cross-linked combinations of hydrophilic and hydrophobic monomers [5]. These micelles self-arrange in shell-like structures with their hydrophilic portion as an outer shell and hydrophobic portion in the central core. Because of their small size, tens of nanometers in diameter, they are ideal for surrounding individual drug molecules.

Hydrophilic outer shells protect the cores and their contents from chemical attack by the aqueous medium in which they must travel. Once the micelles get to the targeted site, drug release is achieved via common polymer degradation mechanisms. Most micelle-based delivery systems are formed from a poly(ethylene oxide)-b-poly(propylene oxide)-b-poly(ethylene oxide) triblock network or a polypeptide and poly(ethylene oxide) combination. These micelles have shown promising results. For example, in one investigation, researchers at the University of Tokyo, led by Kazunori Kataoka, have investigated the use of micelles as a means of delivering doxorubicin (a hydrophobic anticancer agent) [5]. Preliminary results have shown that, when dosed intravenously, the system can stay in blood circulation and effectively deliver the medication to a solid cancerous tumor.

Beyond this, liposomes have been widely examined since 1970 as drug carriers for improving the delivery of therapeutic agents to specific sites in the body [6]. As a result, numerous improvements have been made. Liposomes are lyotropic liquid crystals composed of biocompatible and biodegradable materials. They consist of an aqueous core entrapped by one or more bilayers of natural and/or synthetic lipids. Drugs with widely varying lipophilicities can be encapsulated in liposomes either in the phospholipid bilayer, in the entrapped aqueous core or at the bilayer interface. The compounds entrapped into the liposomes are protected from the action of external media, particularly enzymes and inhibitors. Moreover, liposomes afford a unique opportunity to deliver the drugs into cells by fusion or endocytosis mechanism and practically any drug can

be entrapped into liposomes irrespective of its solubility. With the recent development in the field, several companies are already actively engaged in expansion and evaluation of liposome products for anticancer, antifungal therapy and for prophylaxis. Some of the liposome based products are listed in Table 1.1.

Table 1.1 Liposome-based products in market [6].

Product Name	Drug	Manufacturer
Abelcet	Amphotericin B	The Liposome Company, USA
Amphocil	Amphotericin B	SEQUUS Pharmaceuticals, USA
DaunoXome^{TM}	Daunorubicin	NeXatar Pharmaceuticals, USA
Doxil^{TM}	Doxorubicin	SEQUUS Pharmaceuticals, USA
Doxosome	Doxorubicin	Indian Institute of Chemical Biology, India
MiKasome^{TM}	Amikacin	NeXatar Pharmaceuticals, USA

Nanoparticles (NPs) on the other hand have become more popular because of their specific advantages over liposomes [2]. For example, liposomal formulation is tedious and preparation process is expensive. Along with this there are scale-up problems and difficulty in production of sterile products. There are specific problems with the delivery of liposomes and their contents to the liver such as stability in blood and the degradation of their content following endocytosis [7].

Nanoparticles increase the stability of drugs and possess useful controlled release properties [2]. Modification of physicochemical characteristics of the NP is achievable which cannot be done with liposomes. Various strategies have been

proposed to modify the physicochemical characteristics of the NP which then affects their interactions within a biological environment. For example, changing the chemical nature of the NP can alter certain biological phenomena, such as, biorecognition, biodistribution, bioadhesion, biocompatibility, and biodegradation. Modification of the biological response can also be achieved by incorporation of molecules in the NP. In this case, some of the commonly used molecules are proteins (e.g., albumin, invasins, and lectins) and polymers (e.g., polyethylene glycol, poloxamines, and poloxamers) [2].

1.1.2 Nanoparticles for Drug Delivery

Over the years, variety of synthetic biodegradable polymers, e.g. poly (lactic acid) (PLA), poly (glycolic acid) (PGA), and their copolymers polylactic-co-glycolic acid (PLGA), have been widely explored for the preparation of nanoparticles (Figure 1.1) [8]. In contrast to natural biodegradable polymers (e.g. gelatin, chitosan, albumin), the synthetic polymers are highly pure and reproducible with respect to the monomers ratio and molecular weight (Mol Wt.). Therefore, it allows a greater control and prediction of the degradation kinetics of polymers. These polymers have a long history of human safe usage in surgical sutures and in their usage as raw material for NP preparation.

Polyglycolic acid (PGA)
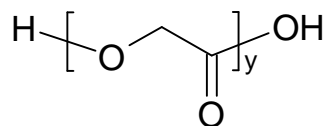
Polylactic acid (PLA)
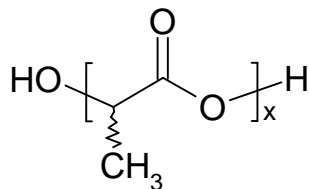
Poly (lactic-co-glycolic acid) (PLGA)
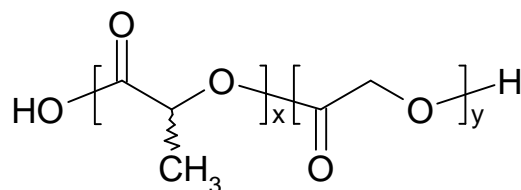
x - Number of units of Lactic Acid
y - Number of units of Glycolic Acid

Figure 1.1 Structural representations of PGA, PLA and PLGA polymers.

The use of biodegradable polymers as drug carriers has long been of interest in controlled release technology because of the ability of these polymers to be reabsorbed by the body. Nanoparticulate delivery system and their use *in vivo* is becoming popular because they promise to overcome many of the obstacles naturally associated with the administration of certain drugs, vaccines, plasmid DNA, and RNAi material [9]. The field of biodegradable polymers is progressing rapidly, so that, researchers now have at their disposal a substantial number of degradable polymers with a range of degradation rates. The most

widely used and studied class of biodegradable polymers is the polyesters, including PLA and PLGA [10]. These colloidal carriers are very useful because they protect incorporated drug against degradation from metabolizing enzymes, modify the drug release profiles, target drugs to specific sites of action (organ or tissue), and deliver biological molecules such as proteins, peptides and oligonucleotides [11]. Qualities of these carriers, like protein protection and control release behavior, are useful for a drug delivery system [12].

Formulation of the polymer for drug delivery system depends on polymers physical properties, for example, Mol Wt., inherent viscosity and mechanical strength influence and control the polymer biodegradation rate and hydrolysis [8]. A wide variety of drugs ranging from small Mol Wt. therapeutic agents to peptides, proteins and hormones, antibiotics and chemotherapeutic drugs, have been successfully incorporated into these biodegradable polymeric nanoparticles [8]. Moreover, it has been proved by fluorescent imaging techniques that nanoparticles have good potential for the encapsulation of plasmid DNA and their use for genetic vaccination seems to be reasonable [13]. Recently, NPs have become popular due to their small size, which allows a transport of carriers across biological membranes thereby improving the transport of the encapsulated molecules [12]. The size of these objects should allow their diffusion out of the blood vessels to reach the pathological areas. In particular, nanoparticles in the size range of 20 - 200 nm have been shown to accumulate preferentially at tumor sites through an enhanced permeability retention effect [2].

NP formulations are promising as drug carriers for the effective transport of poorly soluble therapeutics [14]. The preparation of NPs containing a drug is a challenge that does not normally exist when preparing larger diameter microparticles. The optimal formulation of submicron PLGA particles containing an active agent/drug should satisfy the following: i) small size particles producing a high recovery yield, ii) high encapsulation efficiency and bioavailability of the active agent, iii) minimal 'burst' effect of the effective agent, iv) low levels of toxic agents used in formulation (excluding active agents) v) process scalable to large quantities. In reality, it is difficult to fulfill all the mentioned points; typically compromises are made in at least one of these conditions when preparing NPs [2]. Along with this, different NP formulations have been developed to modify the physicochemical characteristics such as size, structure, morphology, surface texture, and composition [11]. Several encapsulation techniques have already been developed to prepare particulate sustained drug delivery systems [12].

1.1.3 PLGA Properties and Applications

PLGA is a Food and Drug Administration (FDA) approved biodegradable and biocompatible polymer and it became popular because of its resorbability through natural pathways [15]. PLGA co-polymers are aliphatic polyesters composed of varying proportions of lactic and glycolic acids as shown in Figure 1.1. These polymers are available in two forms; either with free carboxylic acid end group (uncapped) or esterified end group (capped). The end group of these

polymers influences the incorporation efficiency and release pattern of loaded drugs.

PLGA nanoparticles protect the therapeutic agent from degradation by physiological conditions, and they release the drug in a controlled manner so that its concentration is maintained within therapeutic levels for longer periods of time [16]. Along with this, these nanoparticles can be made small enough to circulate through capillaries and can cross the highly-permeable vasculature supplying blood to the tumor, and enter tumor cells through endocytosis or receptor-mediated transport. PLGA nanoparticles can specifically target tissues by including targeting moieties in the formulation, and modified to include poly(ethylene glycol) pendant chains for increased circulation time in the vasculature. These favorable pharmacological characteristics result in improved therapeutic efficacy, better use of the pharmaceutical agent, and increased patient compliance and quality of life. These nanoparticles can entrap a wide range of biologically active compounds. Many of the PLGA based drugs are in market, for example, Lupron Depot, Sandostatin, Arestin, Risperidal Consta (Table 1.2) [17]. PLGA nanoparticles are also well suited for vaccine delivery. Numerous proteins, peptides or viruses have been successfully formulated in PLGA particles. Manipulation of physiochemical properties of PLGA NPs is another reason for these particles to become popular. By changing the physiochemical properties, the rate of degradation and release profile can be controlled.

Table 1.2 PLGA-based drugs in market [17].

Product name	Active ingredient	Company	Application
Lupron Depot	Leuprolide acetate	TAP	Prostate cancer
Sandostatin LAR® Depot	Octreotide acetate	Novartis	Acromegaly
Arestin®	Minocycline	Orapharma	Periodontal disease
Risperidal® Consta™	Risperidone	Johnson & Johnson	Antipsychotic

Moreover, it is important to determine if slow or fast degradation rate is needed for targeted delivery of a drug to the diseased tissue [7]. For example, slow proteolysis would be desirable if the transported moiety leaves the target cell on degradation of the vehicle. On the other hand, if the active molecule has to leave the vacuolar system for the cytoplasm in order to be effective, then rapid degradation of the carrier protein is required.

1.1.4 Effect of Physiochemical Properties of PLGA on Degradation

As mentioned before, a major advantage of PLGA co-polymer is the ability to manipulate its physiochemical properties depending on the desired rate of degradation, and subsequently depending on the release profile of the encapsulated drug. The term biodegradable refers to the nonenzymatic, hydrolytic cleavage upon contact of any PLGA device with artificial or biological fluids.

PLGA-hydrolysis produces lactic and glycolic acids (Figure 1.2), which are metabolised in the Krebs cycle to carbon dioxide (CO_2) and water.
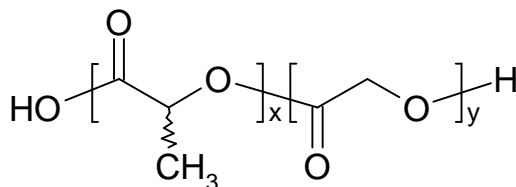
x - Number of units of Lactic Acid
y - Number of units of Glycolic Acid

Poly (lactic-co-glycolic acid) (PLGA)
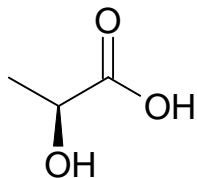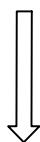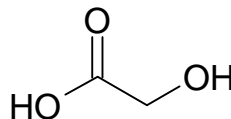
Lactic acid   Glycolic acid

Figure 1.2 Degradation of PLGA polymer through non-enzymatic hydrolysis of the backbone ester linkages.

PLGA degradation happens in two stages. The first stage is degradation, which involves the hydrolytic scission of the ester bonds. The second stage is erosion [18]. PLGA polymer goes through bulk erosion during its degradation. Bulk erosion refers to a biodegradation mechanism where the diffusion of water within the polymer mass is faster than the rate of covalent bond cleavage within the polymer chain. Eventually lactic acid and glycolic acid gets solubilized and the drug gets released. Bulk erosion is favorable for vaccine delivery because it stops

the early release of the vaccine. The rate of PLGA degradation depends mainly on the molecular weight, crystalinity and hydrophobicity of the polymer. Increased rate of degradation is observed with polymers with small molecular weight and that are more hydrophilic [19]. For PLGA, if the ratio of glycolic acid is higher than lactic acid then it will result in increased degradation rate of the polymer because glycolic acid is more hydrophilic than lactic acid. Therefore, PGA has a degradation rate of 2 - 3 months whereas PLA has a degradation rate of 12 - 16 months. One exception to this is that 50:50 glycolic:lactic acid ratio has the fastest degradation rate of 1 - 6 months but mostly it's from 50 - 60 days [17]. This is because of the amorphous nature of 50:50 PLGA. It has the least crystalinity in its structure, thus it is more prone to hydrolysis and degradation than other PLGA polymers with lower or higher glycolic:lactic acid ratios [20]. PLGA end groups also influences the hydrophobicity of the polymer. As mentioned earlier PLGA can have either free carboxylic acid end group (uncapped) or ester end group (capped). Free carboxylic acid end group is more hydrophilic than PLGA with a methyl ester end group. For our study, we used carboxylic end group PLGA because it enhances the polymer and protein/drug interaction resulting in more efficient encapsulation in nanoparticles formulations. Moreover, in contrast to ester terminated PLGA group, carboxylic end group polymer provides stable attachment of polymer to proteins through a covalent bond [21].

1.2. Targeting Hepatocytes

1.2.1 Liver Cells

Four cell types are mainly studied for selective targeting of the drug-conjugate to the liver. These are endothelial cells, kupffer cells, stellate cells and hepatocytes [22]. Endothelial cells are similar in many ways to those of other organs. The difference lies in that these cells contain pores with 100 nm in diameter size. Kupffer cells are scattered between endothelial cells and are very important part of the liver, but are not peculiar to the liver. Stellate cells are also distributed among endothelial cells. Hepatocytes on the other hand make up 70 – 80% of the liver's cytoplasm as shown in Figure 1.3 [22].
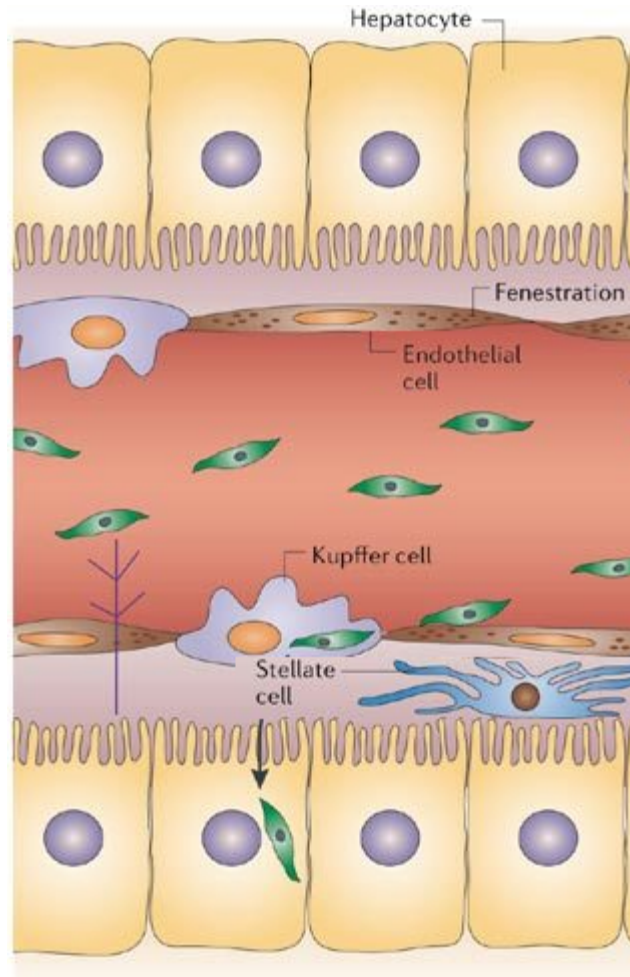
Figure 1.3 Schematic representation of endothelial cells, kupffer cells, stellate cells and hepatocytes [22]. (Adapted from reference [22]).

There are many carbohydrate-specific receptors found on liver cells. These receptors include hepatic receptors, mannose/N-acetylglucosamine receptor, phosphomannosyl receptor and asialoglycoprotein receptor (ASGP-R) [23]. Beyond this, liposome delivery system to the hepatocytes in the presence of an amino acid sequence from the circumsporozoite protein of the Plasmodium sporozoite, a microorganism that displays highly specific and highly efficient targeting to liver, has been studied [3]. Asialoglycoprotein receptor is primarily found in hepatocytes and shows high binding to asialoglycoproteins [24].

13

1.2.2 The Asialoglycoprotein Receptor Lectin

Lectins are proteins that bind to the carbohydrate moieties of glycoproteins and glycolipids [25]. Lectins are widely found in nature, for example in plants, microorganisms, bacteria and animals, therefore they are accessible and can be easily isolated.

The asialoglycoprotein receptor (ASGP-R) lectin was first isolated and characterized in 1971 by Pricer and Ashwell [26]. They observed that the binding capacity of this receptor was highly dependent on sialic acid residues of carbohydrate moiety of ASGP-R. ASGP-R is a transmembrane protein that connects the cell surface to several membranous intracellular compartments. It recognizes galactose-terminated proteins [27]. The asialoglycoprotein receptor is a C-type lectin that binds to asialoglycoproteins with high affinity. It is found primarily in the hepatocytes where it mediates the endocytosis of serum glycoproteins [24, 28].

ASGP-R is responsible for the rapid serum clearance and lysosomal catabolism of desialylated glycoprotein [24]. This receptor has been identified on a continuous human hepatoma cell line, Hep G2. These receptors represent a homogeneous population of high affinity binding sites. Theoretically there are 500,000 surface binding sites per cell on freshly isolated rat hepatocytes [24]. In general, it is illustrated that hepatocytes not freshly isolated may express less receptor protein than freshly isolated hepatocytes [29]. The binding capacity greatly depends on the association of NH_2-terminated amino acid with H1, H2 subunits of

ASGP-R. In previous studies, antibodies have been used against H1 major subunit of the human ASGP-R using synthetic peptide antigens and their binding specificity was confirmed by enzyme linked immunosorbent assay [30]. The existence of ASGP-R in hepatocytes facilitates the feasibility of carrier-directed therapy to the liver. The rate and extent of carrier uptake by hepatocytes is dependent on the size, charge, composition, rigidity and the physicochemical properties of the particles [31]. These characters of abundance, exclusivity and endocytotic function have made the ASGP-R an excellent target for hepatocyte or liver targeted delivery. ASGP-R is responsible for the endocytosis of ligands that are galactosylated or lactosylated.

1.2.3 Ligands Capacity to Bind ASGP-R

The binding capacity between asialoglycoprotein and ASGP-R depends on receptor concentration and association of NH_2-terminated amino acid with H1, H2 subunits of ASGP-R. It has been also shown that galactose, lactose, acetylgalactosamine and asialofetuin have high affinity to ASGP-R. Delivery of galactose-terminated complexes to ASGP-R include asialorosomucoid [32], galactose-terminated neoglycoproteins [33] and asialoglycoprotein [34-35].

A_1-Acid glycoprotein (orosomucoid) is notable from other plasma glycoproteins because of their high abundance of carbohydrate content and large proportions of sialic acid [27, 36]. Removal of the terminal sialic acid residues results in rapid and specific clearance from the circulation by receptor-mediated processes. Sialic acid is *N-* or *O-*substituted derivatives of neuraminic acid, a

monosaccharide with a nine-carbon backbone. After removal of terminal sialic acid residues it is recognized by ASGP-R. Desialylated α_1-acid glycoprotein, asialorosomucoid, has terminal non-reducing galactose residues with a molecular weight of around 40,000 Da. Human α_1-acid glycoprotein contains 5 to 6 acidic asparagines-linked sugar chains per protein molecule. Targeting genes and other agents via the ASGP-R using asialoorosomucoid have been reported [27, 36].

Furthermore, it has been proven that labeling liposomes with asialofetuin (ASF) (natural ligand) greatly enhances liver uptake from 16% to 73% during the first four hours of injection [35]. Based on the above mentioned characterics of ASF, we decided to use ASF as a ligand to target ASGP-R. Asialofetuin (ASF) is a glycosylated protein with complex carbohydrate chains and it has a molecular weight of 48 KDa. ASF has two or more glycans that bind to the hetero-oligomeric subunits of ASGP-R. There are 16 (15 lysine residues plus the amino terminus) reactive amino groups in the asialofetuin (ASF) molecule. Therefore, a carrier containing ASF on the surface should significantly enhance the uptake by hepatocytes.

1.2.4 Endocytosis of Asialofetuin by Hepatocytes

Hep G2 cell line is widely used for studying drug targeting and delivery. Several other human hepatoma cell lines including HepAD38, Huh-5-2 cells are used in anti-hepatitis virus drug-screening. For our purpose, we used Hep G2 cell line as this cell line expresses high number of ASGP-Rs. The number of ASGP-Rs per cell range from 90,000 to 130,000 for Hep G2, 30,000 to 60,000 for

HepAD38 and 20,000 to 40,000 for Huh-5-2 [27]. Moreover, it has been shown that there is a decrease in transfection activity of ASF-complexes in HeLa cells compared to Hep G2 cells [31].

Asialofetuin-ASGP-R is uptaken by endocytosis which is followed by intracellular drug-conjugate cleavage [7]. The term endocytosis includes several mechanisms by which the particles are internalized by cells. The mechanism of asialoglycoprotein uptake by hepatocytes is closely similar to other forms of receptor-mediated endocytosis, particularly to those that show calcium-dependent receptor binding as shown in Figure 1.4. Receptor-mediated endocytosis is a universal mechanism for the uptake of macromolecules by cells. After binding to galactose-terminated molecules, it is transported to lysosomes inside the cell for catabolism and is then recycled [27]. NPs containing asialofetuin get to hepatocytes by passing through the fenestrated endothelium of the sinusoid which has a pore size of 100 nm [37]. Once a receptor-ligand complex migrates into a coated pit, it is internalized in the clathrin-coated vesicle. The endosomes are then fused with lysosomes and their contents are degraded. The ASGP-R is then sent back to the surface of the cell surface to be reutilized and the ligand is catabolized within the body.
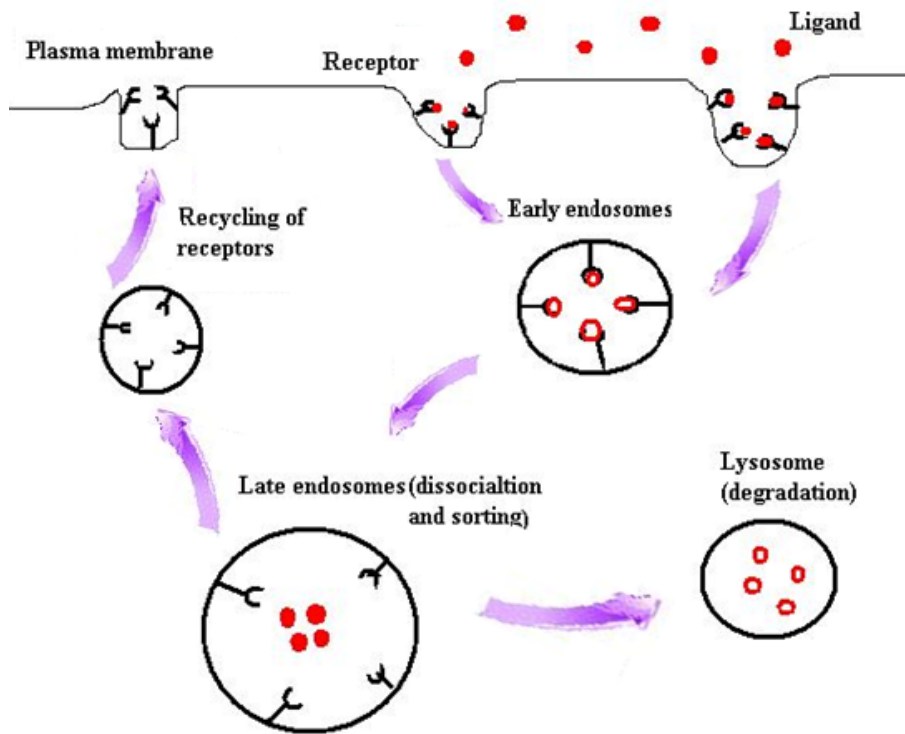
Figure 1.4 Receptor-mediated endocytosis of nanoparticles.

1.3 Targeted Delivery of anti-Hepatitis C Virus Drug to Hepatocytes

1.3.1 HCV and its Discovery

Hepatitis is the inflammation of the liver and viral Hepatitis is the inflammation of the liver resulting from a viral infection [38]. Hepatitis C virus (HCV) was discovered in 1989 by investigators at Chiron, Inc. Before HCV was discovered, hepatitis from blood transfusion that was not caused by hepatitis A or hepatitis B was referred to as non-A, non-B hepatitis. Portions of the HCV genome were isolated by screening complementary diribonucleic acid (cDNA) expression libraries made from RNA and DNA from chimpanzees infected with serum from a patient with post-transfusion non-A, non-B hepatitis. To identify portions of the genome that encoded viral proteins, the libraries were screened

with antibodies from patients who had non-A, non-B hepatitis. These investigators went on to show that the virus they identified was responsible for the vast majority of cases of non-A, non-B hepatitis. They called the new virus HCV. HCV is a positive, single-stranded RNA virus in the Flaviviridae family responsible for acute and chronic liver disease. The genome is approximately 10,000 nucleotides and encodes a single polyprotein of about 3,000 amino acids.

The viral proteins of HCV are divided into structural and non-structural proteins [39]. There are three major structural proteins and several non-structural proteins necessary for viral replication. The structural proteins are the core proteins and envelope proteins which are responsible for the structure of the virus and its ability to gain entry and infect new host cells. The exact function of some of the non-structural proteins is not yet known, it produces new viral particles once it gains entry to host cells. The most targeted structures in the development of therapy approaches are the NS3 protease and the NS5B RNA polymerase [40]. NS3 is a multifunctional protein in which N-terminal contains a serine-like protease and the C-terminus has helicase and NTPase activities [41].

Several different genotypes of HCV with slightly different genomic sequences have since been identified that correlate with differences in response to treatment with interferon alpha [42]. HCV infection is common; it has an average worldwide occurrence of 3%. In about 80% of cases acute HCV infection becomes persistent and may cause chronic hepatitis leading to cirrhosis and, eventually, hepatocellular carcinoma (HCC). HCV-induced end-stage liver disease is currently the leading reason to liver transplant in most western

countries. HCV induces several complex pathways leading to insulin resistance (IR), steatosis, fibrosis, inflammation, apoptosis, and HCC. Because HCV induces these complex pathways, it is believed that these pathways are closely interconnected and it is now proposed that these pathways can be important initiators of HCV pathogenesis. The link between oxidative stress, steatosis and IR is complex, and the exact sequence of events is not clear. Different extrahepatic (for instance adipose tissue or diet) as well as intrahepatic mechanisms have been suggested to explain this interconnection in a more general context. Certainly, IR may lead to steatosis and conversely, steatosis (or more exactly, the accumulation of fatty acid (FA) derivatives used for triglyceride synthesis) can induce IR.

1.3.2 Risk Factors for HCV Infection

Approximately 170 million people worldwide are infected with HCV. Infections based on testing of blood donations worldwide are as high as 500 million [40]. HCV is concentrated in Asia and Africa but a high prevalence is also noticed in North America with an estimated 4 million patients in the United States and 250,000 patients in Canada [43].

The virus is transmitted primarily by blood and blood products [38]. Majority of infected individuals have either received blood transfusions prior to 1990 (when screening of the blood supply for HCV was implemented) or have used intravenous drugs. Contaminated blood transfusion is still a major cause of infection but it has been decreasing because of the emphasis on screening of blood

donors and the advances in screening tests and methods. Currently sharing of contaminated syringes between drug abusers is the major cause of infection.

Other, less common, causes of infection include transplantation of organs, occupational exposure and high risk sexual behavior [39]. HCV infection is rare between monogamous couples but it is more common in sexually promiscuous individuals. Perinatal transmission from mother to fetus or infant is also relatively low but possible (less than 10%). Many individuals infected with HCV have no obvious risk factors. Most of these persons have probably been inadvertently exposed to contaminated blood or blood products [38].

1.3.3 Consequences of HCV Infection

About 80% of individuals acutely infected with HCV become chronically infected, lasting longer than six months [41]. Once chronically infected, the virus is almost never cleared without treatment. The development of chronic HCV infection can vary dramatically between individuals. Some individuals will have clinically insignificant or minimal liver disease with no complications. Others will have clinically apparent chronic hepatitis and some of these people will develop cirrhosis. About 20% of individuals with hepatitis C who does develop cirrhosis will develop end-stage liver disease. Individuals with cirrhosis from hepatitis C are at an increased risk of developing hepatocellular carcinoma (primary liver cancer). Cirrhosis caused by hepatitis C is presently the leading indication for orthotopic liver transplantation in the United States [38].

1.3.4 Diagnosis and Vaccination

The diagnosis of chronic hepatitis C is made by history, serological testing and liver biopsy [38]. Most patients with chronic hepatitis C show asymptomatic or non-specific symptoms such as fatigue. In some individuals, the diagnosis results from blood tests obtained for other reason (usually elevations in the serum alanine and aspartate aminotransferase activities). The development of a vaccine against infection by the Hepatitis C virus has not yet been achieved [44-45]. The reason behind this is the presence of several sub-types of the Hepatitis C virus with major differences between them. Furthermore, hepatitis C infections tend to be chronic because depending on how the virus replicates, there is a constant change in the structure of the virus making it hard to recognize by the immune system and is unable to clear the virus. Moreover, patients who successfully cleared the virus from their system can get infected again if exposed again to the virus. This indicates that the immune system does not efficiently recognize and clear the viral particles.

1.3.5 Liver Transplantation to Cure HCV

Liver transplantation is normally done when antiviral therapy fails or when the diagnosis is done at a late stage of the disease [46]. This approach is expensive and the procedure is complex and long. Even if the operation is successful, it is not always an effective approach as liver transplant does not cure the disease. There is a high chance of re-infection and results in a rapid

destruction of the newly transplanted organ. Therefore the best approach would be to control the viral infection.

1.3.6 Combination of Alpha Interferon and Ribavirin as Antiviral Therapy

Alpha interferon was first approved more than 10 years ago as a therapy for chronic hepatitis C [47]. However this therapy is not effective as it has poor efficacy and is associated with severe side effects. Alpha interferon is a host protein that has natural antiviral activity and is made in response to viral infections. Recombinant forms of alpha interferon have been formed but they are now being replaced by pegylated interferon (peginterferon). Peginterferon is formed by chemically modifying alpha interferon by adding large inert molecule of polyethylene glycol. Pegylation changes the uptake, distribution, and excretion of interferon, therefore, prolonging its half-life. Peginterferon given weekly provides a constant level of interferon in the blood, whereas standard interferon must be given several times a week and provides irregular and fluctuating levels. Furthermore, peginterferon is more active than standard interferon in inhibiting HCV and yields higher sustained response rates with similar side effects.

Ribavirin has been studied for over 20 years as a potential therapy against a number of RNA and DNA viruses, including human immunodeficiency virus, respiratory syncytial virus, parainfluenza virus, lassa fever virus, herpes virus, measles virus and hepatitis C virus [48]. Ribavirin is a broad-spectrum antiviral nucleoside analog of guanosine. The chemical structure of ribavirin is shown in Figure 1.5. It is a synthetic compound that interferes with the viral replication and

life cycle. Ribavirin alone has little effect on HCV, but combined with interferon increases the sustained response rate by two- to three-fold.
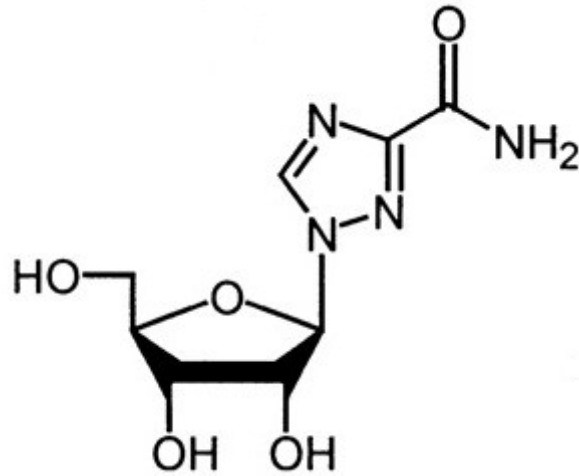
Figure 1.5 Chemical structure of ribavirin [49]. (Adapted from reference [49]).

Therefore, combination therapy is recommended for hepatitis C, and interferon monotherapy is only applied when there are specific reasons not to use ribavirin [42, 47]. Another reason for using combined therapy is that the relapse rate is lower for combined therapy compared with monotherapy. A 48-week course of combination therapy using peginterferon and ribavirin yields a sustained response rate of about 55% whereas a similar course of peginterferon monotherapy yields a sustained response rate of only 35%. A response is considered "sustained" if HCV RNA remains undetectable for 6 months or more after stopping therapy. Pilot studies show much more promising results when twice-daily ribavirin (1000/1200 mg/day) is added to interferon-alfa therapy (3 MU thrice weekly), resulting in improvement in end-of-treatment and end-of-follow-up responses [48]. Combination therapy with peginterferon alfa and ribavirin has demonstrated high

sustained viral response rate and likewise low rates of virologic relapse in large clinical trials.

There are few drawbacks to this therapy. One is the high cost associated with this therapy [39]. Currently, to treat one of the genotypes of the virus, it costs $25,000 US for a 48 week course of therapy. It is estimated that in US the direct medical costs of Hepatitis C therapy will exceed $10 billion US by the next decade. Another drawback to this therapy is that there are many side effects associated with this therapy. The most common side effects are flu like symptoms and fatigue. This is believed to be largely related to interferon. The other common side effects resulting from interferon include a decrease in the white blood count and decrease in platelet count (a blood clotting element). The least common effects resulting from interferon include depression, irritability, sleep disturbances, nausea and anxiety as well as personality changes. Generally these effects are controllable but it requires fair amount of counseling with the patients. The most significant side effect of ribavirin is hemolytic anemia. Other side effects with ribavirin include cough and some shortness of breath. Rare side effects resulting from ribavirin may include rash. There is also the risk of birth defects; therefore ribavirin is not given to someone who is pregnant or is considering becoming pregnant.

To overcome these drawbacks, we can selectively target this combination therapy to the hepatocytes using asialoglycoprotein receptor. As mentioned before, this receptor is predominantly expressed on the sinusoidal surface of the

hepatocytes. Selective targeting will result in reduction in side effects, low dosage of the drug taken daily and improvement in efficacy.

1.3.7 Current Formulations for Targeting Hepatocytes

A number of formulations are being studied for targeting hepatocytes, some of them are discussed below. Extensive research has been done on the asialoglycoprotein receptor present on mammalian hepatocytes for the development of liver-specific carriers, such as liposomes, recombinant lipoproteins, and polymers for drug or gene delivery to the liver, especially to hepatocytes [50]. The use of asialofetuin, or synthetic ligands with galactosylated or lactosylated residues, such as galactosylated cholesterol, glycolipids, or galactosylated polymers have achieved significant targeting efficacy to the liver. Development of efficient targeted drug delivery system into cells is very crucial for the improvement of drug carriers [3]. Targeting of nanoparticle systems are in vogue since past few years. For therapeutic purposes, targeted delivery is important to lower the adverse implications on healthy tissue, especially for tumor-related therapies, which generally involve delivery of cytotoxic compounds, nuclear medicines, or toxins. For both diagnostic and therapeutic aspects, it is important that the delivery attributes remain the same upon subsequent application and are not significantly changed by the body's immune system. Targeting liver heparan sulfate proteoglycans with liposome containing a lipid-anchored 19-amino acid glycosaminoglycan peptide and encapsulated drug has proved to be an efficient mechanism of delivering nanoparticle contents

beyond the liver sinusoidal region and into hepatocytes [3]. The system has multiple advantages that make it apt for targeting drugs to liver tumor regions. The risk of cardiotoxicity from doxorubicin in cancer therapy is lowered as a result of very low amounts reaching the heart. The particles are able to transcend endothelial hurdles and release the contents in the parenchymal areas of the target organ. The stability of the particles is enhanced with polyethylene glycol and delivery features remain unaltered with repeated administration [51].

Chitosan nanoparticles made by ionic gelation have an important role in drug delivery for use in medical formulations because of its biocompatibility, biodegradability, enhanced transfection efficiency, and low toxicity [52]. But this system is significantly limited by its low cell specificity. Glycyrrhizin (GL) surface modification of ligand conjugated chitosans has proved to increase the efficacy of hepatic targeting. The ionic gelation method, however, has a few limitations like particle aggregation due to instable physiological pH and also being unsuitable for intravenous administration. To overcome the limitations ,GL surface-modified *N*-caproyl chitosan nanoparticles (NCC) made by periodate oxidation method has been used as an alternative. The nanoparticles using NCC molecules possess more enhanced dimensional and GL surface-binding stability and slow release characteristics in plasma *in vitro*. This suggests that hydrophobic caproyl groups do not allow hydrogen bonding and prevent aggregation. Tissue distribution studies showed NCC-NPs-GL are more efficiently accumulated in the liver compared with non-GL modified NCC-NPs. In addition, more NCC-NPs-GL is taken up by the hepatocytes in the liver,

reflecting NCC-NPs-GL stability and being a suitable vehicle for safe hepatocyte-targeting.

Ribavirin, an antiviral drug, is an approved therapeutic for Respiratory Syncytial Virus infection particularly in children [53]. Chronic hepatitis C is treated with this broad spectrum drug in conjunction with interferon. However the mechanism of action has not been understood well thus far. Extensive research suggests ribavirin to be a prodrug which must be metabolized *in vivo* to be an active pharmacological agent. It has some limitations though as a therapeutic of hepatitis. The primary adverse effect of the drug is development of anemia which may be detrimental to a cardiac patient. This happens as a result of the accumulation of ribavirin 5- triphosphate in the red blood corpuscles (RBC) which is a metabolite of ribavirin. Attempts have been made for more targeted delivery of ribavirin to the liver and minimizing metabolite accumulation in the RBC thus increasing the therapeutic potential and minimizing side effects. Viramidine, earlier known as ribamidine, has been reported to be an important compound which has the characteristics of ribavirin. Research shows viramidine is converted to ribavirin in the liver so it may be an important hepatic targeted precursor of ribavirin. *In vitro* and clinical studies seem to suggest viramidine as a next generation ribavirin with enhanced potential.

Although several formulations have been used to target hepatocytes using different strategies, our goal is to target hepatocytes using asialoglycoprotein receptor. As mentioned earlier, asialoglycoprotein receptor is highly expressed in hepatocytes and asialofetuin shows high binding to this receptor.

1.3.8 PLGA Nanoparticle Preparation Methods

The choice of a particular method of drug encapsulation is mainly determined by the desired size range of NPs needed for targeting specific cell type as well as drug solubility considerations. NP size of 100 nm or less can easily penetrate through the sinusoidal endothelial cell fenestrae reaching the hepatocytes [31, 35]. Moreover, a method that can give high encapsulation of hydrophilic drug, like ribavirin, is required [11, 15, 54-56]. Double emulsion technique is mostly used for encapsulation of hydrophilic drugs. Various methods have been prepared to increase the encapsulation of hydrophilic drugs inside NPs [11, 15, 54-56]. Furthermore in order to increase the encapsulation efficiency, when entrapping the drug, addition of Ca^{2+} in the molar ratio of 2:1 of calcium to drug (alendronate) has been used in primary emulsion. Ca^{2+} is used to reduce the solubility of the drug in water. It has been shown that addition of calcium increases the encapsulation but addition of too much calcium reduces the entrapment efficiency. Molar ratio of 2:1 gives the best results. The pH of NP formulation is another factor that can affect entrapment efficiency. Encapsulation is higher at pH 7 and lower at pH 5 [54].

1.4 Hypothesis and Objective

1.4.1 Hypothesis

Polylactic-co-glycolic acid nanoparticles (PLGA NPs) surface coated with asialofetuin (ASF) can selectively target hepatocytes as these cells express high levels of receptor for asialofetuin.

1.4.2 Objective

The objective of this thesis is to prepare ASF-coated PLGA nanoparticles for targeted delivery to hepatocytes. Our efforts to achieve this objective are described in the following chapters.

First, two different methods were used to prepare double emulsion PLGA NPs, namely, double emulsion solvent evaporation method and emulsification diffusion method. Secondly, ASF was coated to the surface of NPs using covalent conjugation, followed by labelling the protein with rhodamine. Finally, these ASF coated NPs were used for *in vitro* cell uptake studies using Hep G2 cell line.

CHAPTER 2. Experimental Methods

2.1 Materials and Equipment

Polylactic-co-glycolic acid (50:50) with carboxylate end group, Mol Wt. 7000 Da, was purchased from Durect Corporation Birmingham USA. Ethyl acetate, acetone and chloroform were purchased from Caledon Laboratories Ltd. Georgetown Ontario Canada. Micro BCA protein assay kit was purchased from Fisher Scientific Corp, USA. Bradford kit was purchased from BioRad laboratories Inc. Hercules, CA. Asialofetuin type 1 (Mol Wt. 48 KDa), bovine serum albumin (Mol Wt. 66 KDa), dimethyl sulfoxide, propylene carbonate (PC), didodecyldimethylammonium bromide (Mol Wt. 462.63), and 5(6)-carboxy-X-rhodamine N-succinimidyl ester (Mol Wt. 631.67, Ex. 575 nm, Em. 605 nm) were purchased from Sigma. Dialysis tubing, 3500 Da, was purchased from Fisherbrand. 1-Ethyl-3-(3-dimethylaminopropyl) carbodiimide hydrochloride (Mol Wt. 191.70) and N-hydroxysuccinimide (Mol Wt. 115.09) were purchased from Fluka. Tripson-EDTA and Dulbecco's Modified Eagle Medium was purchased from Biochemistry store, University of Alberta. Reagent A and B for Lowry assay were supplied by Dr. Ayman El-Kadi, Faculty of Pharmacy and Pharmaceutical Sciences, University of Alberta (Reagent B, Folin-Ciocalteu's, was purchased from Sigma, Aldrich and reagent A was prepared using 1 mL of 1% $CuSO_4$, 1 mL of 2% Na.K.Tartarate and 20 mL of 10% Na_2CO_3 anhydrous in 0.5 M NaOH).

PLGA NPs were sonicated using ultrasonic processor XL2010 (Farmingdale, NY). Centrifugation of NPs was done using Avanti J-20XP Beckman coulter USA. PLGA NPs were freeze dried using VirTis from SP Industries, Stone Ridge, NY. Average diameter and size distribution of the NPs was obtained by dynamic light scattering using Malvern Zetasizer 3000HS (Malvern Instruments Ltd, UK). NPs prepared using emulsification diffusion method was homogenized using a homogenizer (Ika ultra-Turrax T25, Germany). The size of dry NPs was also measured using humidity Bioscope™ Atomic Force Microscope (Digital Instruments, Santa Barbara, CA), Hitachi H700 transmission electron microscope and JEOL 6301F field emission scanning electron microscope. For SEM the sample was coated with gold using a Nanotech SEM Prep 2 DC sputter coater. NPs were centrifuged using the centrifuge (biofuge ISR Heraeus Instruments) to remove physically adsorbed unbound asialofetuin from NPs. The absorbance of physically bound asialofetuin on NPs was measured at 595 nm using ELISA reader (Versa max microplate reader). Labeling of asialofetuin with rhodamine was measured using a Kodak imager 4000MM. For cell study, detachment of the cells from the surface of the flask was viewed under the microscope (Leitz Diavert microscope transformer model 2-D, Guelph, Canada). The cells were centrifuged using the centrifuge (biofuge 15R, Heraeus Instruments). The uptake of the ASF-NP sample by Hep G2 cells was observed under the fluorescent microscope (Axio observer, Carl Zeiss Canada Ltd, Ontario, Canada) and flow cytometry (Becton-Dickinson Facsort).

2.2 Preparation of PLGA Nanoparticles (NPs)

2.2.1 Preparation of NPs using Double Emulsion Solvent Evaporation (DESE) Method

Poly(D,L-lactic-co-glycolic acid) (PLGA) NPs were prepared by modification of the DESE method reported by Diwan et al. [57-58]. In general, PLGA (100 mg) was dissolved in chloroform (200 µL). To make single emulsion, PBS (100 µL, 10 mM, pH 7.4) was added to the PLGA solution and was sonicated using ultrasonic processor for 15 seconds at medium-high speed. Double emulsion was made by transferring PVA/PBS (2 mL, 9%) into the suspension and sonicating it for 45 seconds at medium-high speed. The resulting emulsion was transferred drop-wise into PVA/PBS (8 mL, 9%) and allowed to stir for 3 hours. The sample was transferred into a 40 mL centrifuge tube followed by centrifugation at 19,000 rpm for 15 minutes at 4 °C. NPs were washed twice with sterile water (30 mL) at 19,000 rpm for 15 minutes and then were re-dispersed in sterile water (2 mL). Subsequently, the suspension was transferred to the vial and freeze dried over 2 – 3 days.

2.2.2 Characterization of NP Prepared using DESE method

Average diameter and size distribution of the NPs prepared using DESE method was obtained by dynamic light scattering (DLS) using Malvern Zetasizer. NPs (1 mg) were dissolved in distilled water (4 mL) from which 3 mL was transferred to the cuvette. The cuvette was placed in the instrument sample

compartment, which was at ambient temperature (25 °C) during the measurement. During the laser-illuminating step, the movement of the particles was measured, and the diameter and size distribution was calculated.

The size and morphology of the NPs was further confirmed using scanning electron microscope (SEM). Briefly, 0.1 mg of PLGA NP was scattered over SEM stub with conducted carbon tape. The sample was then gold coated and observed under the scanning electron microscope.

2.2.3 Preparation of NPs using Emulsification Diffusion (ED) method

A literature procedure [15] was used for the preparation of PLGA NPs using ED method. Changes were made to the reported method to obtain appropriate size of the NPs. In general, PLGA (50 mg) was dissolved in polycarbonate (PC, 2 mL) or ethylacetate (EA, 2 mL) solvent. The solution was then added to Didodecyldimethylammonium bromide (DMAB, 10 mL, 3%) and was emulsified for 7 minutes at 22,000 rpm using the homogenizer. To the emulsion, distilled water (40 mL) was slowly added under moderate stirring. After overnight stirring, solvent was removed by dialysis (3500 Da) in water twice, 18 and 5 hours. Subsequently, the suspension was transferred to the vial and sample was freeze dried over 2 – 3 days to obtain ~300 mg of NPs.

2.2.4 Characterization of NP prepared using ED method

Average diameter and size distribution of sample before and after freeze drying were measured with a dynamic light scattering particle sizer, Zetasizer.

NPs before freeze drying will be referred as "NP solution" and NPs after freeze drying as "dry NP". To measure the size of NPs in NP solution, sample (3 mL) was transferred to the cuvette. Whereas, the sample for dry NP was prepared by dissolving dry NPs (1 mg) in distilled water (4 mL), from which 3 mL was transferred to the cuvette. The diameter and size distribution was obtained as mentioned before (Section 2.2.2).

The size and morphology of dry NP was also measured using atomic force microscope (AFM), transmission electron microscopy (TEM) and scanning electron microscope (SEM). Briefly, AFM experiment was carried out by placing an aliquot (2 µL) of the nanoparticular solution (0.1 mg/mL) on a freshly cleaved mica surface (flogopite, $KMg_3AISi_3O_{10}(OH)_2$) and air dried at room temperature. Sample was imaged in air at room temperature using humidity Bioscope™ Atomic Force Microscope. An integral silicon tip cantilever (OMCL-AC160TS-W2, Olympus Cantilevers) with a spring constant of 10 pN/nm was used. AFM tapping mode imaging was done at scan rates of 1 – 1.5 Hz/line and set point of 600 mV. All images were processed with a second-order flattening routine for background correction. Various fields within the same stub were monitored and recorded. The images were digitally scanned and recorded in graphical electronic file format.

To observe the image under TEM, an aqueous droplet of nanoparticulate solution (20 µL) with a polymer concentration of 2 mg/mL was placed on a copper coated grid. The grid was held horizontally for 1 minute to allow the colloidal aggregates to settle. A drop of 2% solution of phosphotungstic acid

(PTA) in PBS (pH 7.0) was then added to provide the negative stain. After 1 min, the excess fluid was removed by filter paper. The samples were loaded into a Hitachi H700 TEM. Images were obtained at a magnification of 28 K.

The morphology and size distribution using SEM was obtained as before (Section 2.2.2).

2.2.5 Stability of NPs upon Storage

NP solution (4 mL) that was prepared using ED method (Section 2.2.3) was kept in glass vials at 4 °C and -20 °C. The size of these PLGA NPs was then monitored at different time intervals over two months period using the Zetasizer. The NP solution used for storage experiments was in PBS (10 mM PBS, pH 7.4). This is because NPs prepared in the beginning using ED method were dialyzed in PBS, and not in water.

2.3 Non-Covalent Adsorption of Asialofetuin (ASF) on PLGA NPs

2.3.1 Labeling of Asialofetuin with Rhodamine

Asialofetuin (10 mg) was dissolved in sodium bicarbonate (1 mL, 50 mM, pH 8.5) and was kept on ice. In a separate vial, activated rhodamine (5(6)-Carboxy-X-rhodamine N-succinimidyl ester, 1 mg) was dissolved in DMSO (1 mL) which was then slowly added to the protein solution. The ASF and rhodamine mixture was left to react for 2 hours on ice. Un-reacted rhodamine was removed by dialysis (3500 Da) in PBS (1 L, 10 mM, pH 7.4) for overnight at 4 °C

36

[59]. After dialysis, labeled protein (~2 mL) was transferred into a vial and stored at 4 °C.

2.3.2 Characterization of Rhodamine labeled Asialofetuin using Kodak Imager

Different dilutions of the rhodamine labeled asialofetuin sample obtained above (Section 2.3.1) were prepared as shown below in Table 2.1.

Table 2.1 Serial dilutions of ASF-rhodamine were prepared for fluorescence imaging.

Sample number	Sample* (µL)	
	NP-ASF	**Water**
1	20 µL from sample	0
2	10 µL from sample 1	10
3	10 µL from sample 2	10

*Sample (ASF-rhodamine from Section 2.3.1)

Each sample (10 µL) was spotted on a parafilm and was observed using the Kodak imager 4000MM, set at wavelengths for excitation at 575 nm and emission at 605 nm.

2.3.3 Physical Adsorption of Labeled Asialofetuin on NPs

NPs (0.6 mg) prepared using ED method (Section 2.2.3), were dispersed in phosphate buffer (600 µL, 10 mM, pH 5.0). In a different vial, rhodamine labeled ASF (~0.5 mg) was dissolved in PB (100 µL). Protein was allowed to adsorb onto

the NP at 4 °C for 18 hours [60]. The sample was centrifuged at 10,000 rpm for 15 minutes to remove any unbound protein. NPs were washed twice with PBS (pH 7.4, 10 mM) at 10,000 rpm for 15 minutes and then were re-dispersed in PBS (1 mL). Bradford and Lowry assays were performed to determine the protein concentration of the NPs [60].

2.3.4 Characterization of Asialofetuin coated NPs using Bradford Assay

Bradford assay was used to determine the protein (ASF) concentration of the NPs. Bovine serum albumin (BSA) was used as a standard. A series of standard solutions of BSA (0, 50, 100, 200, 400, 600, 800, 1000 µg/mL) were prepared. Bradford solution was prepared by mixing Bradford reagent and water (1:3.75). Bradford solution (190 µL) and standards (10 µL) or samples (10 µL) were added on an ELISA plate. The plate was incubated for 2 hours at 37 °C. After 2 hours, the absorbance was measured at 595 nm using ELISA reader. A linear plot was obtained for absorbance versus concentration of the standards as shown in Figure 2.1. Then the concentration of the sample was calculated using the standard curve.
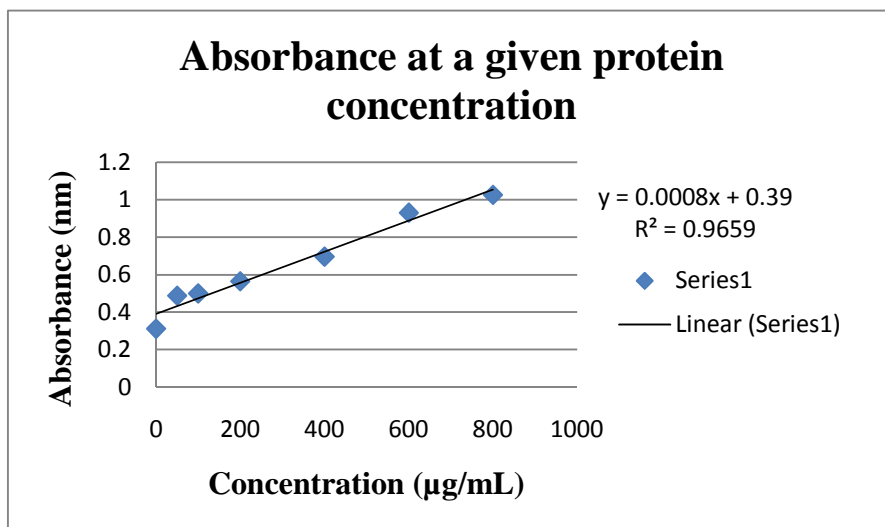
Figure 2.1 standard curve of absorbance versus concentration for Bradford assay.

2.3.5 Characterization of Asialofetuin coated NPs using Lowry Assay

Protein (ASF) concentration of NPs was also determined using Lowry assay. A series of standard solutions of BSA (0, 100, 200, 300, 400, 500 µg/mL) were prepared. Sample dilutions were prepared as shown below in Table 2.2.

Table 2.2 Different concentrations of NP-ASF-rhodamine were prepared for fluorescence imaging.

Dilution	Sample* added (µL)	Water added (µL)
1	10	240
2	50	200

* Sample (NP-ASF-rhodamine from Section 2.3.3)

Standard solutions (250 µL) and samples (250 µL) were mixed with 250 µL of reagent A (200 µL of 1% $CuSO_4$; 200 µL of 2% Na.K.Tartarte and 4 mL of 10% Na_2CO_3 anhydrous in 0.5 M NaOH) and was left for 10 min at room temperature. Under continuous vortex, 750 µL of reagent B (1/10 diluted solution of Folin-phenol reagent) was added to each of the standard solution and the solutions were left in the water bath at 50 °C for 10 minutes. Then 200 µL from each tube was transferred to the ELISA plate to analyze using ELISA reader at 550 nm. A linear plot was obtained for absorbance versus concentration of the standards as shown in Figure 2.2. The concentration of the sample was obtained from the standard curve.
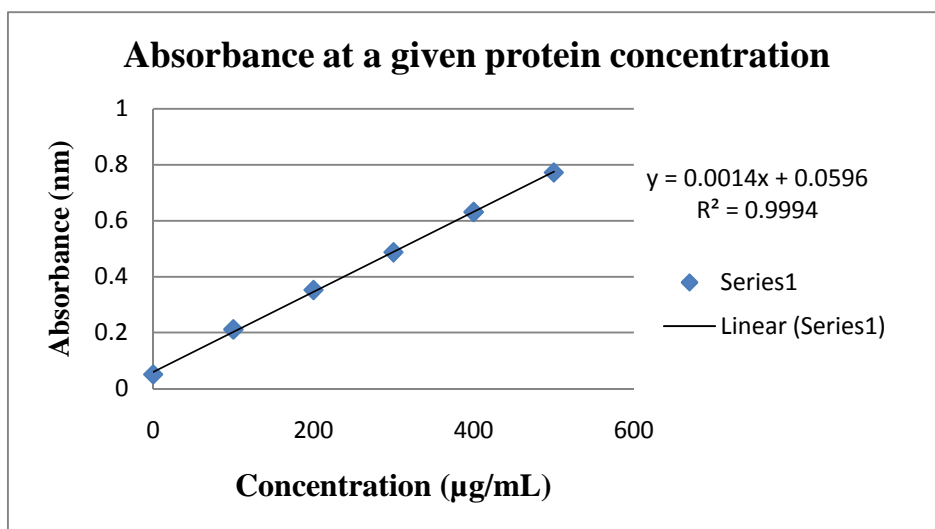
Figure 2.2 standard curve of absorbance versus concentration for Lowry assay.

2.4 Covalent Binding of Asialofetuin (ASF) on PLGA NPs

2.4.1 Covalent Conjugation of Asialofetuin on Nanoparticles

NPs were covalently conjugated to ASF using the method described by Kalkanidis, M et al. [61]. NPs (~75 mg, which is ¼ of the freeze dried NPs from section 2.2.3) were dissolved in sterile water (1.25 mL). EDC (200 µL of 50 mg/500 µL) was added to react with the carboxylic acid group of the NPs to form an intermediate, o-acylisourea. The intermediate was reacted with NHS (165 µL of 1.5 M) to form an acylamino ester. Finally, MOPS (500 µL of 500 mM, pH 6.5) and sterile water (2.385 mL) were added to the reaction vessel and the mixture was stirred for one hour at room temperature. Subsequently, activated NPs were reacted with ASF (2 mg) to form a stable covalently linked conjugate. The mixture was further stirred overnight at 4 °C. Glycine (175 µL of 7 mg/mL) was then added and the mixture was allowed to stir for 30 minutes. At the end, sample was centrifuged at 20,000 rpm for 25 minutes at 4 °C, (Rotor type = 25.50) to remove any unbound protein. Conjugated NPs were washed twice with PBS (pH 7.4, 10 mM) at 20,000 rpm for 25 minutes and were re-dispersed in PBS (1 mL). NPs were then freeze dried for 24 hours to obtain protein conjugated (NP-ASF) nanoparticles (~28 mg). BSA (negative control) was conjugated to the NPs using the same procedure.

2.4.2 Characterization of NP-ASF using Bicinchoninic Acid (BCA) Assay

Protein concentration of the ASF-conjugated (NP-ASF) NP was determined by BCA assay using the manufacturers protocol. A series of standard

solutions of BSA (500, 250, 125, 62.5, 31.25, 15.63, 7.81, 3.91, 1.95, 0.98, 0.49, 0 µg/mL) were prepared. The NP samples were prepared as shown in Table 2.3.

Table 2.3 Preparation of samples for characterization of the NP-ASF.

	Sample (mg)	Water (µL)
Empty NP	5	500
NP-ASF	5	500
NP-ASF	2.5	500
NP-ASF	1.25	500
NP-BSA	5	500
NP-BSA	2.5	500
NP-BSA	1.25	500

The BCA reagent (500 µL, 25:24:1, Reagent MA:MB:MC) was added to each tube and was incubated for about 50 minutes in the water bath set at 55 °C. Then the tubes were removed from the water bath and were left at room temperature for an hour to cool off. Next, the tubes were centrifuged for 20 minutes at 14,000 rpm using a microcentrifuge. The supernatant (200 µL) was transferred to a 96-well microtiter plate and the plate was read using a plate reader at 562 nm.

2.4.3 Labeling of NP-ASF with Rhodamine

NP-ASF was labeled with rhodamine using the method described by Hermanson G et al. [59]. A solution of rhodamine, 5(6)-Carboxy-X-rhodamine N-

succinimidyl ester (1 mg in 500 µL DMSO) was slowly added to NP-ASF solution (~28 mg in 1 mL water from section 2.4.1). The sample was stirred overnight at 4 °C. Un-reacted rhodamine was removed by centrifugation at 14,000 rpm for 20 minutes. Labeled NPs (NP-ASF-rhodamine) were washed with PBS (pH 7.4, 10 mM) at 14,000 rpm for 20 minutes and then were re-dispersed in PBS (1 mL). The sample was freeze dried for 24 hours.

2.4.4 Characterization of NP-ASF-rhodamine NPs using Kodak Imager

The extent of fluorescence labeling of NP-ASF-rhodamine sample was estimated using Kodak imager. A standard curve for rhodamine was first obtained. Rhodamine (1 mg) was dissolved in DMSO (1 mL) to prepare a stock which was further diluted as shown in Table 2.4.

Table 2.4 Standard rhodamine samples prepared using known concentration of 5(6)-Carboxy-X-rhodamine N-succinimidyl ester for fluorescence imaging.

Sample number	Sample (µL)		Net Intensity	Mean Intensity
	Rhodamine	**Water**		
1	5 µL from stock*	35	4087429	1192.8
2	20 µL from sample 1	20	3844840	661.6
3	20 µL from sample 2	20	1991006	454.9
4	20 µL from sample 3	20	871498	290.9
5	20 µL from sample 4	20	365521	216.0
6	20 µL from sample 5	20	120433	142.9

* Stock: 1 mg Rhodamine was dissolved in 1 mL DMSO

Different dilutions of the NP-ASF-rhodamine solution obtained above (Section 2.4.3), after the sample was freeze dried, were also prepared as shown in Table 2.5.

Table 2.5 Serial dilution of NP-ASF-rhodamine NPs for fluorescence imaging.

Sample number	Sample	Dilution	Water (µL)	Net Intensity	Mean Intensity
1	NP-ASF	1 mg	500	808146	138
2	NP-ASF	250 µL from sample 1	250	508393	108
3	NP-ASF	250 µL from sample 2	250	429030	100
4	NP-BSA	1 mg	250	1070226	121
5	NP-BSA	250 µL from sample 4	500	932813	112
6	NP-BSA	250 µL from sample 5	250	538648	99
7	Rhodamine	1 mg	500	3711797	167

Standard rhodamine or NP-ASF-rhodamine, 10 µL each, were spotted on a parafilm and the fluorescence intensity of each spot was measured using the Kodak imager set at wavelengths, excitation 575 nm and emission 605 nm. Rhodamine concentration in NP-ASF and NP-BSA was estimated based on the fluorescence of control rhodamine sample (Table 2.5) and not the standard curve (Table 2.4). Standard curve was not used as the intensity changes from one experiment to another, and these experiments were done on different days.

2.5 Cellular Uptake Studies

2.5.1 Cell Line Culture

Hep G2 cells, a generous gift from the laboratory of Dr. Ayman El-Kadi, University of Alberta, were thawed under aseptic conditions by first gentle agitation in the water bath at 37 °C for 2 minutes. Hep G2 was cultivated at 37 ℃ in a 5% CO_2 incubator. It was cultured in DMEM media with 1% L-glutamine, and 10% FBS (Invitrogen, Karlsruhe, Germany), 100 IU/mL penicillin, and 100 IU/mL streptomycin. The thawed cells were transferred to a 75 cm^2 tissue culture flask containing DMEM media (15 mL) and were incubated at 37 °C. The media was changed after 2 days. After 5 days when Hep G2 cells reached confluence, cells were used for uptake study using fluorescent microscope and flow cytometry.

2.5.2 Uptake of NP-ASF-Rhodamine by Cells using Fluorescent Microscopy

For uptake study, the media was removed from the flask and cells were incubated with trypsin (3 mL) for 5 minutes at 37 °C to detach cells from the surface. The adherent cells were viewed under the microscope to check whether all the cells have detached from the surface. Media (10 mL) was added to the flask and gently pipetted to ensure cell clumps were broken and a homogeneous mixture was formed. Then the cells were transferred to centrifuge tube (15 mL) and were centrifuged for 7 minutes at 1600 rpm. Supernatant was discarded and the pellet was suspended in fresh media (10 mL) containing serum until

homogeneous mixture was formed. From this 100,000 cells were transferred to each well in a 2-well chamber slide. The cells were incubated with media (3 mL) for overnight. Then NP-ASF-rhodamine or NP-BSA-rhodamine (0.5 mg or 1 mg) was dissolved in media (500 µL) and the solution was added to each of wells in the chamber slide and was incubated for 2 and 4 hours. NP-BSA-rhodamine was used as a negative control. Washing was done by removing the media and by adding PBS (3 mL) buffer for 5 minutes at room temperature. Cells were washed 3 times. Sample (cells) was observed under the fluorescent microscope.

2.5.3 Uptake of NP-ASF-Rhodamine by Cells using Flow Cytometry

Hep G2 cells were prepared in DMEM media containing serum as described above (Section 2.5.2). Cells (1 million) were incubated at 37 °C in a 6-well plate with media (3 mL) for 2 hours. Then NP-ASF-rhodamine or NP-BSA-rhodamine (0.5 mg or 1 mg) was added to each well and the plate was incubated overnight. Cells were next washed by removing the media, and were detached from the surface of the 6-well plate with a scrapper. Media (10 mL) was added to the wells and was pipetted up-down to make a homogeneous mixture. The cells were transferred to centrifuge tube (15 mL) and were centrifuged for 7 minutes at 1600 rpm. Supernatant was removed and FBS/PBS (1 mL, 10%) buffer was added and was pipetted up-down to make a homogeneous mixture. Around 500,000 cells were taken for flow cytometry. The data was analyzed using Dako cytomation summit software.

2.5.4 Competitive Study

Hep G2 cells were prepared in DMEM media containing serum as described above (Section 2.5.2). Cells (1 million) were incubated in a 6-well plate with media (3 mL, 37 °C) for 2 hours. ASF (0.5 mg) was then added to the cells and incubated for overnight. Next day, NP-ASF-rhodamine (1 mg) was added to cells and cells were incubated for another four hours. Finally, cells were washed by removing the media and were prepared as described above (Section 2.5.3) for the flow cytometry experiment.

CHAPTER 3. Results and Discussion

3.1 Preparation of PLGA Nanoparticles

The choice of method for the preparation of PLGA nanoparticles (NPs) was dependent on two important parameters. First, the NPs will be used for encapsulation of a hydrophilic drug: i.e, the anti-HCV drug ribavirin. Secondly, the desired NPs will target hepatocytes. Double emulsion, solvent evaporation (DESE) technique was chosen for the preparation of NPs because this method gives better encapsulation of the hydrophilic drugs in NPs. The double emulsion consists of three fluid phases. The outer and inner phases are aqueous and the middle phase consists of a hydrophobic layer. The schematic of such a double emulsion PLGA NP is shown in Figure 3.1.
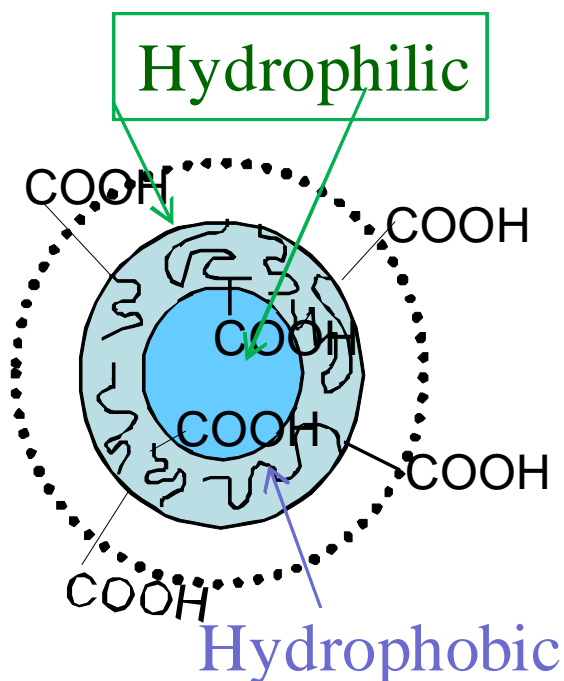
Figure 3.1 Schematic representation of double emulsion PLGA NP.

In order to penetrate through the sinusoidal endothelial cell fenestrae and reach hepatocytes, the size of particles should be less than 100 nm [35]. Two methods were used to prepare PLGA NPs to satisfy this size requirement. The first method was DESE method. While DESE method allowed the preparation of double emulsion NPs, smaller size NPs of less than 100 nm was not obtained. A second method, emulsification diffusion (ED) method was used to prepare double emulsion NPs of the desired size range.

3.1.1 Double Emulsion Solvent Evaporation (DESE) Method

The DESE method for the preparation of PLGA NPs is a popular method for the microencapsulation of peptides, proteins, and hydrophilic drugs [62]. DESE method has been used for the purpose of prolonging the release of drugs. This method also allows easy control of particle size and scale-up. However, there are some limitations in the use of this NP preparation method. For instance, proteins might be altered to some extent by interfaces and agitation stress with this method. Other disadvantages are difficulty and necessity of removal of solvent and surfactant (which can be toxic), low particle yield, too many steps for the preparation, and necessity of usage of a lot of surfactant (e.g. polyvinyl alcohol) for the preparation of small sized particles. The surfactant present on the surface of the particles is difficult to remove. It is known that polyvinyl alcohol (PVA) on the surface of NPs change the biodegradabililty, biodistribution, and drug release behavior of drug carrier. Along with this, surfactants can cause side-reactions such as an allergy-like reaction [63].

Double emulsion was prepared by dissolving PLGA in an organic solvent (step 1) which was then poured into first aqueous phase (PBS) to give w/o emulsion. After sonication, second aqueous phase (surfactant) was added to the w/o emulsion. The emulsion was further sonicated or homogenized which resulted in double emulsion (w/o/w) as shown in Figure 3.2.
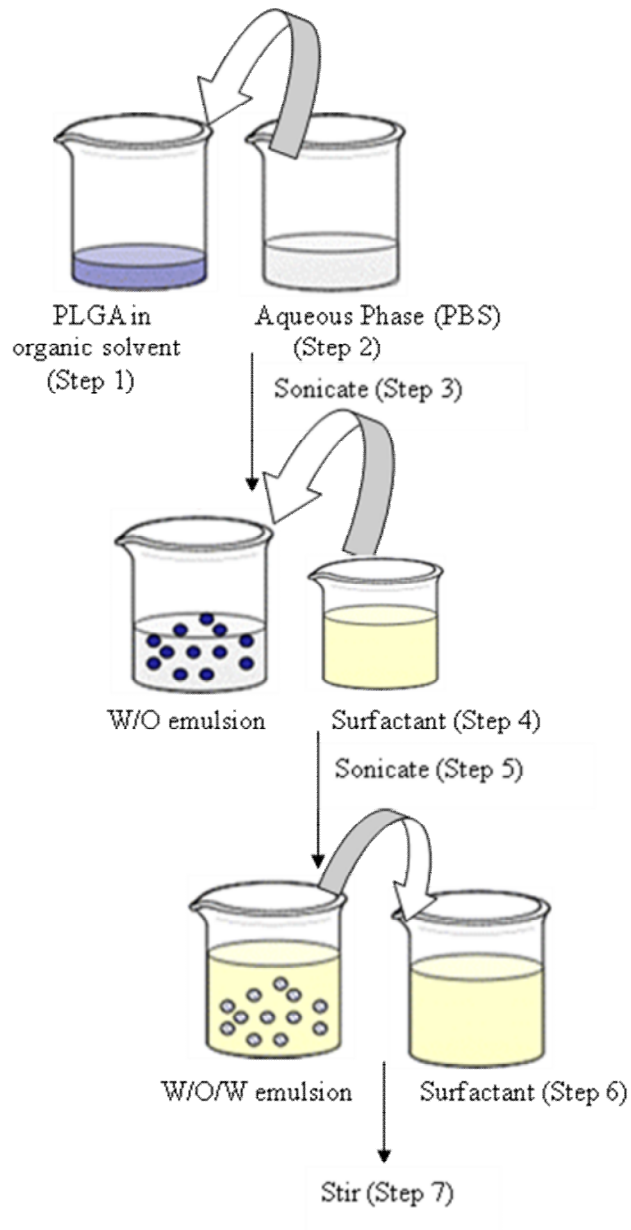
Figure 3.2 Schematic representation of DESE method.

After complete solvent evaporation by stirring, NPs were obtained by centrifugation, followed by washing with cold deionized water, and freeze-drying. The lyophilized NPs were suspended in water to characterize their size using Zetasizer. In general, NPs of size range 644 ± 56 nm were obtained. Figure 3.3 shows that the size of NPs (699 ± 25 nm) obtained using DESE method for a representative sample. The experiment was repeated twice but still the size was much larger than the desired size of NPs (~100 nm).
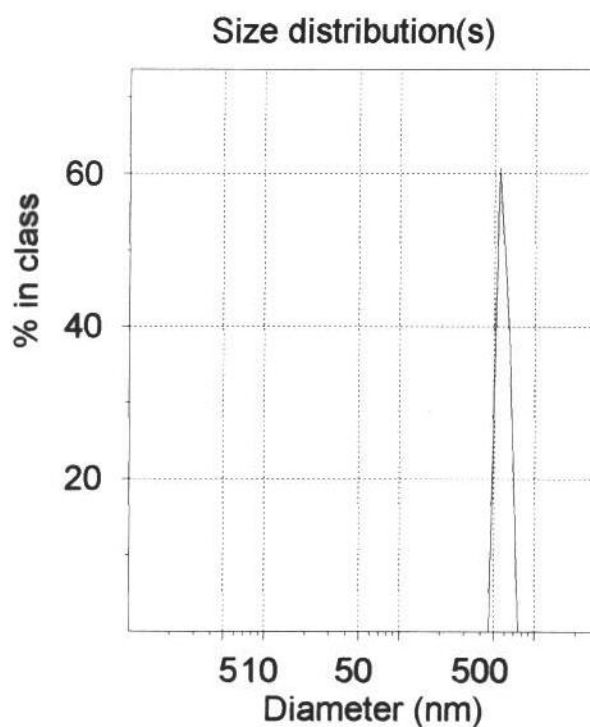
Figure 3.3 Size distribution of PLGA NPs prepared using DESE method.

A number of variations were made in the DESE method in order to obtain NPs with desired size range, such as decrease in the amount of surfactant, increase in sonication time, solvent change and different methods to evaporate the solvent.

Figure 3.4 illustrates how the NP size varies with respect to variations (1-5) made to the DESE method.

Solvent: Influence of the solvent (variation 1), such as chloroform or dichloromethane (DCM), in the organic phase during NP formation is an important factor that affects the size. In the original DESE method, PLGA was dissolved in chloroform. When chloroform was replaced with DCM, an increase in NP size (1262 ± 359 nm) was observed as shown in Figure 3.4. The experiment was done twice and both times similar size range was obtained. Sahana et al have shown that DCM gives larger size particles compare to that of when chloroform is used as a solvent [64]. Size distribution of 1008 ± 12 nm using Zetasizer for one of the experiments with variation 1 is shown in Figure A1 (appendix).

Physicochemical properties of polymer and solvents, such as the ability of the polymer to solublize in the solvent, viscosity of solvents and polymer can affect the size [65]. When the affinity between the solvent and the polymer is higher, it results in supersaturation and therefore, large NPs are formed [55]. Moreover, solvents that have high affinity for water tend to promote solvent diffusion and polymer chain partition into the aqueous phase. In general, broad range of NP mean sizes occur for solvents that have high affinity to water [11].

The reason for smaller NP size with chloroform could be because the affinity of the chloroform for PLGA is lower compared to the affinity between DCM and PLGA. Chloroform has a solubility of 1 g in 200 mL in water at 25 °C whereas DCM has a solubility of 1 g in 50 mL in water at 25 °C [64].

Sonication time: Sonication time (variation 2) is another factor that affects the size of PLGA NPs. It was observed that with slight increase in sonication time, the size of NPs decreased. When sonication time was increased from 45 seconds to 60 seconds, the size of NPs decreased to 528 nm ± 26 nm (Figure 3.4). Size distribution of 547 ± 10 nm using Zetasizer is shown in Figure A2 (appendix). The experiment was done twice and both times the size range was similar.

Stirring vs vacuuming: The organic solvent was removed from the NP emulsion by either stirring at room temperature or vacuuming off the solvent (variation 1). It was concluded from the two experiments that vacuuming increases the size to (1262 ± 359 nm) as shown in Figure 3.4. Size distribution of 1008 ± 10 nm using Zetasizer is shown in Figure A1 (appendix). This could be because vacuuming is not as gentle and therefore can result in aggregation of NPs. Also, it is known that the decrease of nanoparticle mean size correlates with increase of magnetic stirring rate [15]. Mixing by mechanical shear stress of magnetic stirring decreases the particle size.

Surfactant: Surfactant PVA is used to stabilize NPs as surfactant prevents NPs from aggregation. However, surfactant use should be limited to the minimum level to avoid possible toxic and hypersensitivity reactions [18]. A decrease in NP size was observed with the decrease in volume of the surfactant (variation 3, the experiment was done twice) from 8 mL to 4 mL while keeping the concentration

constant (9% PVA/PBS). NPs of size range 356 ± 79 nm were obtained. Size distribution of 412 ± 10 nm using Zetasizer is shown in Figure A3 (appendix). But one must be careful as low surfactant content in the aqueous phase can result in very heterogeneous emulsions of NPs. In general, the higher the concentration of surfactant used, the smaller the mean NP size (9% surfactant used to prepare NPs gives smaller NP size compared to 1% surfactant used). An increase in the NP size (1176 nm $\pm$ 28 nm) was observed when 1% PVA/PBS (variation 4, the experiment was done twice) was used instead of 9% (Figure 3.4). Size distribution of 1156 ± 10 nm using Zetasizer for one of the experiments with variation 4 is shown in Figure A4 (appendix). NPs of size range (358 ± 50 nm) were obtained when large volume of DCM (5 mL), 1% PVA/PBS (20 mL) and increase in sonication time (variation 5, the experiment was done six times) was used. Size distribution of DESE method with variation 5 using Zetasizer is shown in Figure A5 (308 ± 10 nm).
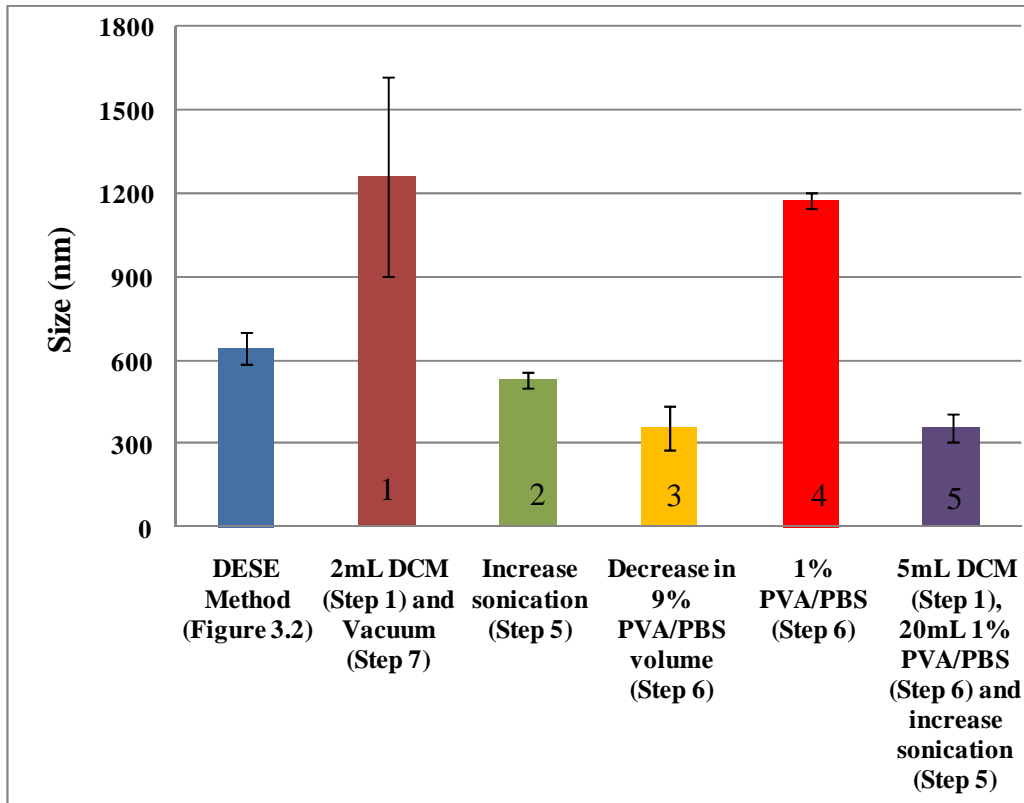
Figure 3.4 Size distribution of the NPs prepared using DESE Method. Variations were made (1-5) with respect to the original DESE method shown in Figure 3.2. *The error bars represents standard deviation.

In general, NPs with size around 300 nm was the lowest that was achieved which was still larger than the desired size of NPs. These results suggest that DESE method may not be the method of choice for the preparation of PLGA NPs with size less than 100 nm.

The size of freeze dried NPs was further confirmed using scanning electron microscopy (SEM). An image of NPs prepared used DESE method is shown in Figure 3.5. The SEM image shows that the particles are spherical and are 350 ± 50 nm in size. This size range is consistent with the size of NPs obtained using the Zetasizer.
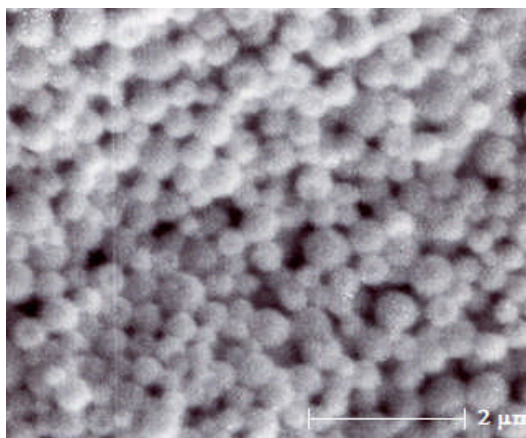
Figure 3.5 Scanning electron microscope (SEM) image of the PLGA nanoparticles (freeze dried) prepared using DESE method. The image shows the shape and the size distribution of NPs.

3.1.2 Emulsification Diffusion (ED) Method

A second method that was used for the preparation of NPs was Emulsification Diffusion (ED) method. It has been shown that ED method gives NP of the size range around 100 nm [15]. ED method is of particular interest because of the use of non toxic solvents. This method is efficient, easy to implement, and scale up is easy. Further, it is highly reproducible with narrow size range, and formation of NPs does not require high stress shear, meaning sonication speed does not need to be high [59]. Disadvantages of this process are that it requires large amounts of water for NP preparation, the size is highly sensitive to polymer concentration and entrapping hydrophilic drugs is still a challenge. This is because hydrophilic components have a high migration tendency to the aqueous phase and thus the drug entrapment efficiency is low.

NPs were prepared using ED method by dissolving PLGA in propylene carbonate (PC) which was then poured into first aqueous phase (surfactant). The

56

surfactant used here was didodecyldimethylammonium bromide (DMAB) instead

of PVA. After homogenization, second aqueous phase (water) was added drop-

wise to the w/o emulsion to obtain w/o/w double emulsion as shown in Figure 3.6.
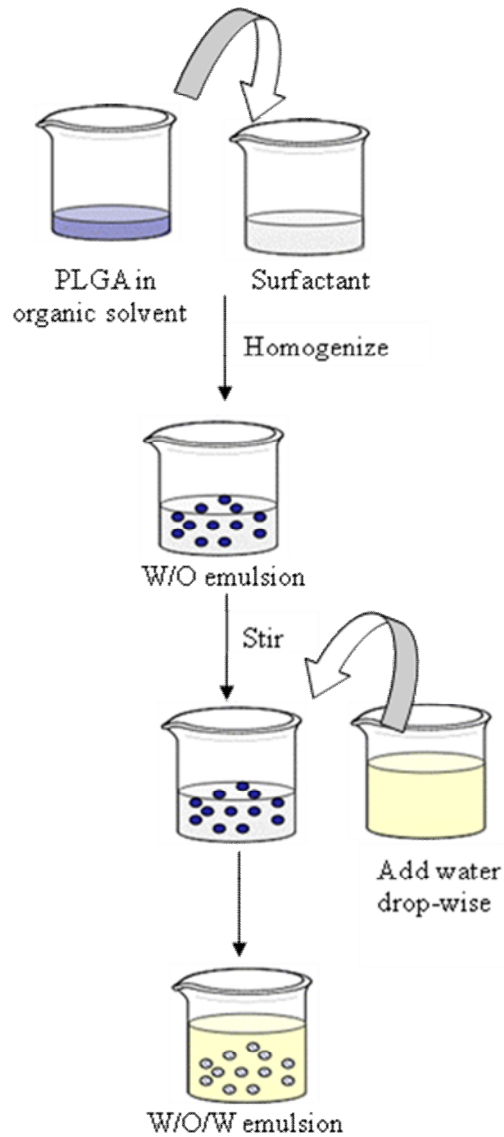
Figure 3.6 Schematic representation of ED method.

NP size distribution was characterized using Zetasizer. Figure 3.7 shows

the size of PLGA NPs prepared using ED method. The size of PLGA NPs was

measured before freeze drying (Figure 3.7 a) and after freeze drying (Figure 3.7 b)

and was found to be 90 ± 15 nm and 305 ± 12 nm, respectively. The size increases

after freeze drying most likely due to aggregation.
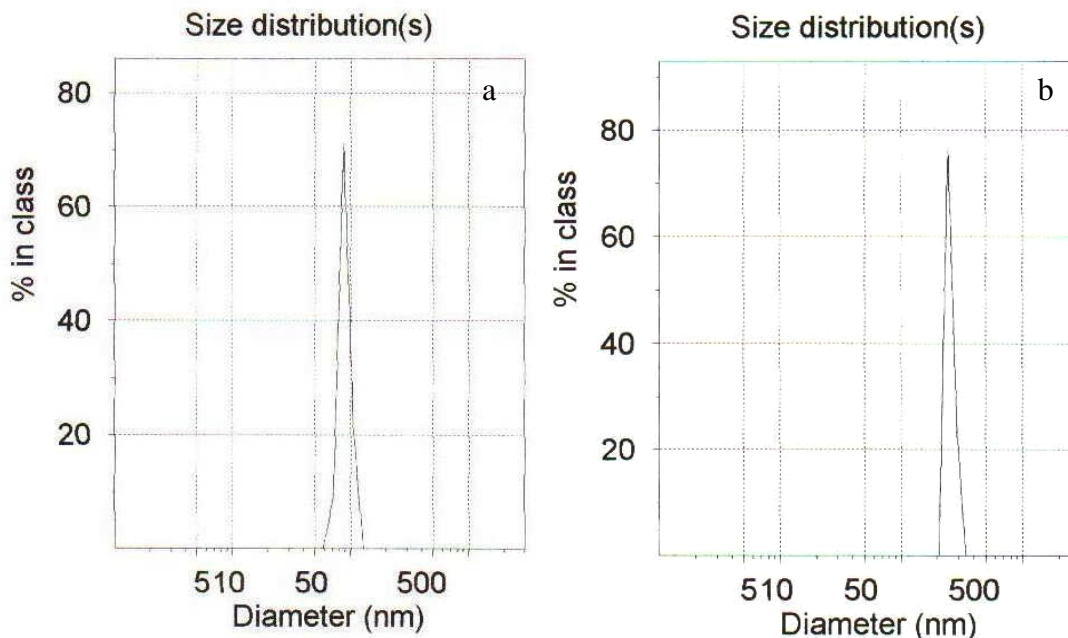
Figure 3.7 Size distribution of PLGA NPs before freeze drying (a) and after freeze drying (b) prepared using ED method. The size was measured using Zetasizer.

The method gave the desired size of NP when the NP solution was not

freeze dried. In addition, changes were made in the ED preparation method, as

performed for DESE method, in order to further reduce the size of NP to be less

than 100 nm after freeze drying. Figure 3.8 illustrates how the size changes with

respect to changes made to ED method. It was observed that surfactant,

homogenization rate, solvent and freeze drying affect the size of the PLGA NPs.

Surfactant: For the preparation of NP using ED method, DMAB was

used as a stabilizer instead of PVA. It has been shown that the mean particle size

of nanoparticles prepared using DMAB results in a smaller size than that of PVA [15]. Normally, high concentration of surfactant use results in smaller NP size. It was found that 3% DMAB gives the smallest size using ED method, therefore, 3% DMAB was used in all our future NP preparations.

Homogenizer rate: Homogenizer rate is another factor that affects the size of PLGA NPs. The homogenization of the oil-in-water emulsion is crucial step in the formation of NPs. In general, decrease of NP mean size corresponds with an increase of homogenizer speed. A speed of 16,000 - 22,000 rpm was used to prepare NPs, and above 25,000 rpm there was no reduction of particle size as reported by Kwon et al. [15]. Therefore, homogenizer speed of 22,000 rpm was used to prepare PLGA NPs.

Solvent and freeze drying: The type of solvent used to prepare NPs can affect the mean size as observed previously in the DESE method. For ED method, we studied the effect of ethyl acetate (EA) and propylene carbonate (PC) on the mean size of PLGA NPs. The NP prepared using PC as a solvent was found to be in the size range of 103 ± 12 nm before freeze drying (the experiment was repeated ten times) and 229 ± 76 nm after freeze drying (the experiment was repeated eight times) (Figure 3.8). However, NP prepared using EA as a solvent was found to be 115 ± 20 nm before freeze drying (experiment was done four times) and 478 ± 73 nm after freeze drying (experiment was done six times) (Figure 3.8). From one of the experiments, size distribution of NP prepared using

59

PC as a solvent is shown in Figure 3.7 (90 ± 15 nm before freeze drying and 305 ± 12 nm after freeze drying). Size distribution of NP prepared using EA as a solvent is shown in Figure A6 (109 ± 20 nm before freeze drying and 394 ± 15 nm after freeze drying). Freeze drying is crucial for the storage of NP for a long period of time because the dry state offers increased stability due to the reduced conformational flexibility, therefore, less potential for structural perturbations [18]. But it is vital to use the right method of freeze drying as choice of poorly developed drying method results in instability or aggregation of insufficiently stabilized particles.

Cryoprotectants, such as ethylene glycol, propylene glycol and glycerol, are used to stabilize the formulation during freezing whereas lyoprotectants, such as trehalose, sucrose, maltose and lactose, stabilizes the formulation during drying [66]. These disaccharides sugars are more effective than monosaccharides like glucose or larger saccharides like maltohexaose. Most commonly trehalose or sucrose is used to stabilize the formulation because both are non-reducing sugars and can act as both cryo- and lyo-protectants. They provide a glassy matrix by remaining amorphous during freeze drying. Moreover, Tamber et al. noticed complete elimination of peptide aggregation when they used mannitol or lactose as cryoprotectant [18]. An acceptable freeze-dried product can be formed by freezing the formulation at the temperature lower than the collapse temperature (Tc) [67]. Above Tc, which is usually about 2 °C higher than glass transition temperature in the frozen state, the product loses its macroscopic structure and collapses during freeze drying. Tang et al. in their paper suggested that a small safety margin of 2

°C can be used if the sample is freeze-dried for more than 2 days, a large safety margin of 5 °C can be used if the sample is freeze-dried for 10 hrs, and a safety margin of 3 °C can be used if the sample is freeze dried anywhere between 10 hrs to 2 days.
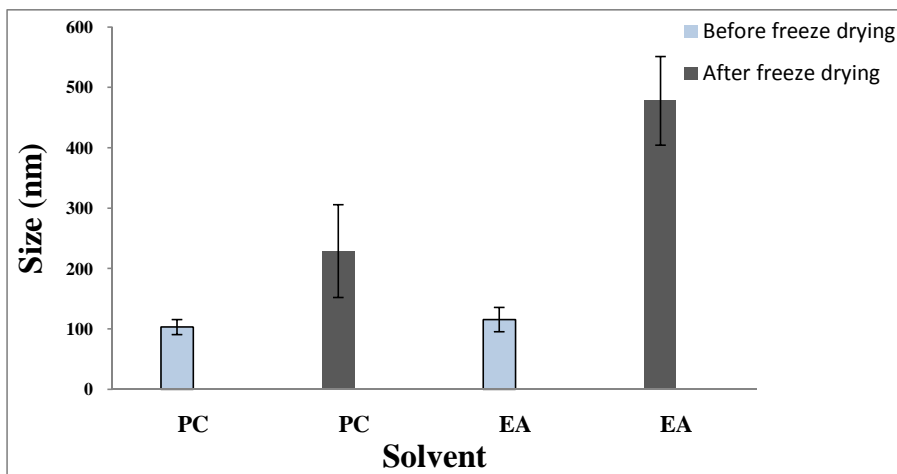
Figure 3.8 Characterization of the NP size prepared using different organic solvents during ED Method. PC, propylene carbonate; EA, ethyl acetate. The error bars represents standard deviation.

The size of freeze dried NPs was further confirmed using imaging techniques such as atomic force microscopy (AFM), transmission electron microscopy (TEM) and scanning electron microscopy (SEM). The AFM image (Figure 3.9 a) shows that the particles are spherical and are in the size range of 200 ± 30 nm. The AFM picture proves that the size increases after freeze drying. TEM also shows the particles are spherical and have size in the range of 200 nm (Figure 3.9 b). The SEM image obtained for the NPs prepared using the ED method shows appearance of aggregates in the background as shown in Figure 3.9 c. In contrast, a really good SEM image was obtained for the NPs prepared using

DESE method (Figure 3.5). Despite repeated attempts using the SEM or TEM techniques, a good image for the NPs prepared using ED method was not obtained. Nevertheless Figures 3.9 b and c show that particles were spherical and were in the size range of 200 ± 50 nm. The reason for not getting a good image could be because in this method dialysis was used instead of centrifugation to remove the surfactant, and it is possible that dialysis does not remove the surfactant effectively and causes the particles to aggregate.
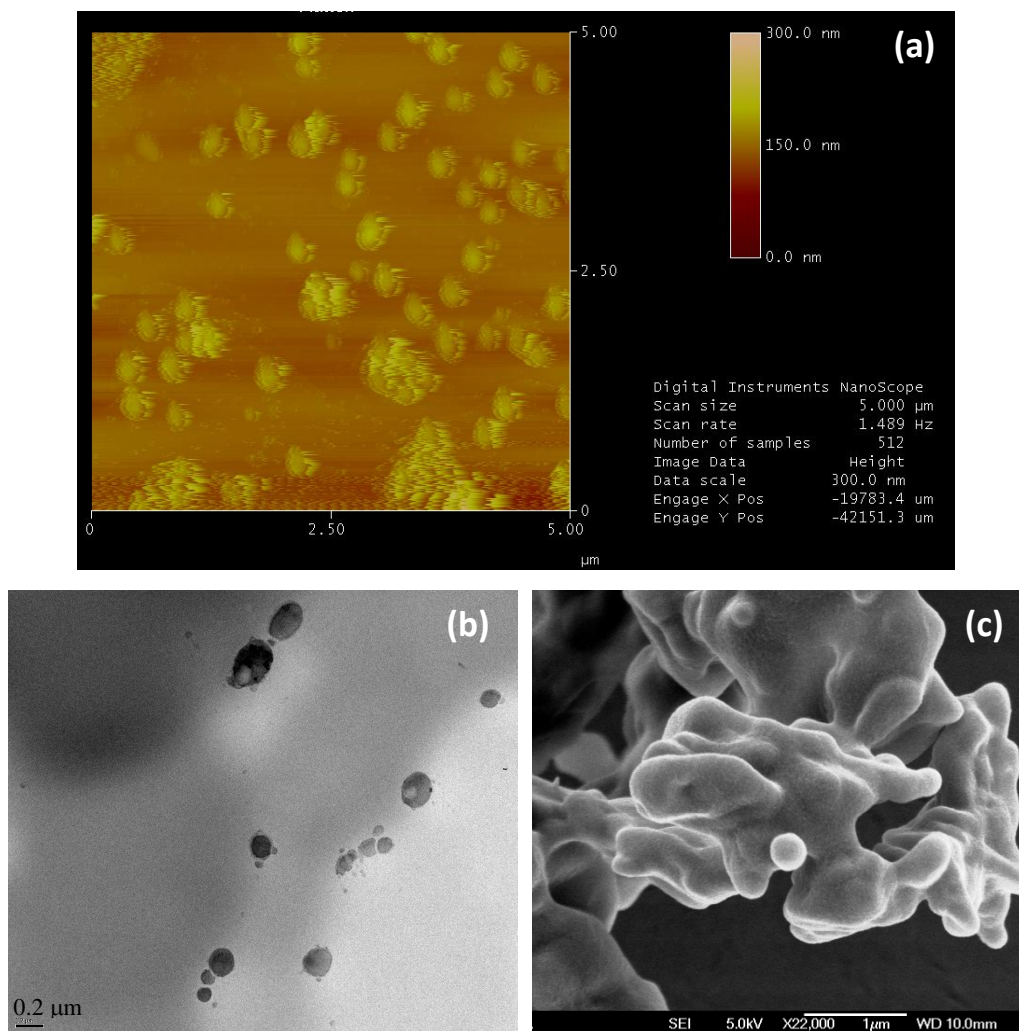
Figure 3.9 Size distribution of freeze dried PLGA nanoparticles for ED method using (a) Atomic force microscope, (b) Transmission electron microscope and (c) Scanning electron microscope.

3.1.3 Storage of NPs in Solution at Different Temperatures

Next, we explored the stability of NPs in solution when stored over a long period of time at 4 °C and -20 °C. The stability of size was monitored for NPs in solution as NPs seem to maintain small size in solution. NP solution was stored at 4 °C in a refrigerator and the size was measured using Zetasizer at different time intervals. NPs seem to maintain size for up to 21 days, after which the NPs started to precipitate out of solution as shown in Table 3.1.

Table 3.1 Stability study on NPs in solution prepared using ED method (organic solvent PC) and stored in the refrigerator at 4 °C.

Time (hrs/days)	PLGA NP Size* (nm)
2 hrs	185
20 hrs	174
2 days	177
4 days	181
15 days	185
21 days	181
39 days	429 (precipitate)
61 days	aggregated

*The size of these nanoparticles is slightly larger (at t=2hrs) as stability experiment was performed on PLGA nanoparticles prepared originally (without the modification of solvent, homogenization time and centrifugation time).

When stored at -20 °C, the NP solution was frozen. After thawing, the NPs showed a dramatic increase in size (Table 3.2). The samples were stored at -20 °C for 2 and 20 hours and the increase in size was observed after 2 hours suggesting NP aggregation upon freezing the NP solution. The experiment was, therefore, not continued.

63

Table 3.2 Stability study on NPs in solution prepared using ED method (organic solvent PC) and stored in the freezer at -20 °C.

Time (hrs)	PLGA NP Size (nm)
2	420
20	368

3.2 Non-Covalent Adsorption of Asialofetuin (ASF) on PLGA NPs

Non-covalent or physical adsorption of ASF on PLGA NPs was done in two steps which is described in the following sections. Physical adsorption results by interaction between the NP surface and the functional groups present on the protein without forming a chemical bond. The advantage of physical adsorption is that this method allows the protein to adsorb on to the NPs without changing any basic properties of the protein.

3.2.1 Labeling of Asialofetuin with Rhodamine

Biomolecules, such as peptide/protein labeled with fluorescent molecule, allow us to study cellular localization and interaction with other molecular and cellular components [1]. Proteins can be labeled with any of a number of different fluorescent probes currently available from commercial sources. Each probe option has its own characteristic spectral signals of excitation (or absorption) and emission (or fluorescence). Many derivatives of these fluorescent probes possess reactive functional groups convenient for covalently linking to proteins and other molecules. Each of the main fluorophore families contains at least a few different

choices in coupling chemistry to direct the modification reaction to selected functional groups on the molecule to be labeled. These choices include amine-reactive, sulfhydryl-reactive and aldehyde-reactive. In choosing a fluorescent tag, the most important factors to consider are good absorption, stable excitation, and efficient, high-quantum yield of fluorescence. Some fluorophores, such as fluorescein, exhibit fluorescence quenching, which lowers the quantum yield over time. Up to 50% of the fluorescent intensity observed on a fluorescein-stained slide can be lost within 1 month of storage.

For this project, activated rhodamine with the N-hydroxy-succinimidyl-ester (NHS-ester) functional group was used for labeling the protein asialofetuin. NHS-ester derivative has greater specificity toward primary amines in the presence of other nucleophiles and results in a more stable linkage following labeling [68]. NHS-Rhodamine is an amine-reactive fluorescent labeling reagent that absorbs green visible light (542 nm) and emits orange-red visible light (575 nm). Rhodamine displays lower sensitivity to pH than fluorescein and is more photostable; however, rhodamine conjugates have a significantly lower quantum yield than fluorescein conjugates. N-Hydroxysuccinimide (NHS)-ester labeling reagents are the simplest and most commonly used reagents for labeling proteins. Proteins, including antibodies, generally have several primary amines in the side chain of lysine (K) residues that are available as targets for NHS-ester reagents.

Asialofetuin (ASF) was conjugated to activated NHS-rhodamine ester at 0 °C for 2 hours (Step 1, Figure 3.10). Un-reacted rhodamine was removed by dialysis in PBS for overnight at 4 °C [59]. The fluorescence intensity of rhodamine

labeled ASF was measured using Kodak imager. After successful labeling, the protein was adsorbed onto PLGA NPs as shown in Figure 3.10 (Step 2). Surface modification of PLGA NPs with ASF was done in order to increase the interaction between the biomaterial (PLGA NP-ASF) surface and the biological environment (receptors, such as ASGP-R) without changing the mechanical properties of the base biomaterial.
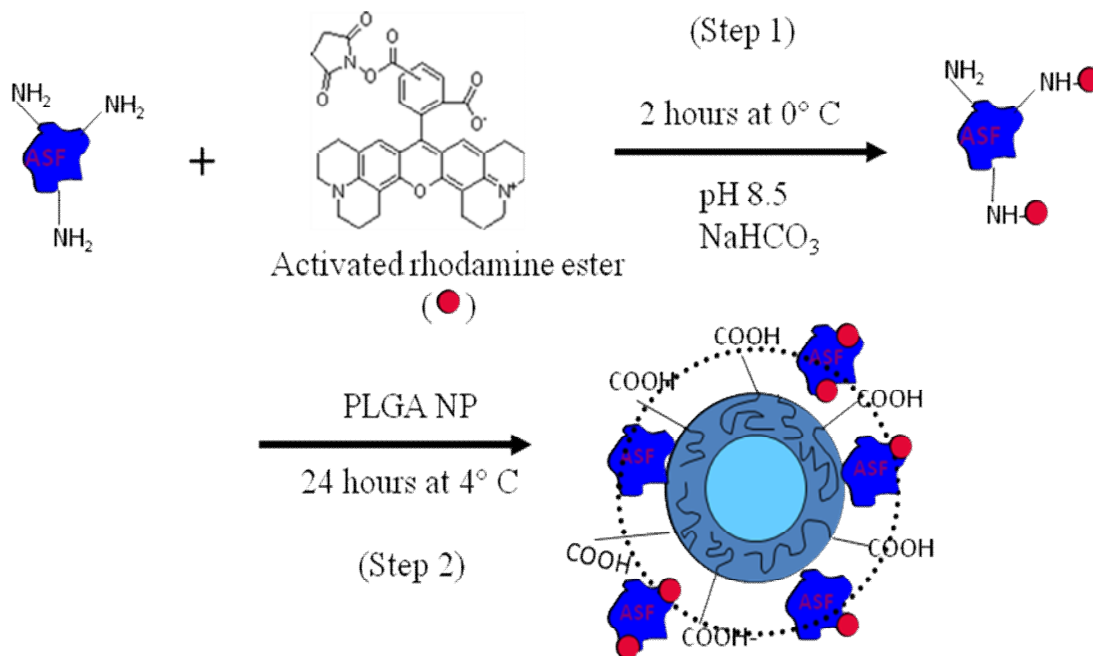
Figure 3.10 Schematic representation of step wise non-covalent adsorption of ASF on PLGA NPs. (● **= rhodamine**)

Rhodamine labeled ASF was imaged using Kodak imager and the protein was found to be labeled with rhodamine as shown in Figure 3.11. Small aliquots of the stock solution (5 µL, 10 µL and 20 µL) were spotted on a parafilm and each spot displayed good fluorescence intensity. The final fluorescence/protein ratio was found to be dependent on many factors such as: pH, dye-protein ratio, reaction temperature and molecular weight of the protein.

pH: In order to maintain the high conjugation efficiency and to maintain the native conformation and the activity of the proteins, the NHS ester and protein reactions are preferred at the mildly basic pH [69]. The higher the pH of the reaction mixture, the stronger intensity of the fluorescence is obtained. NHS esters react efficiently with primary amino groups ($-NH_2$) in pH 7 - 9 buffers to form stable, covalent amide bonds. Therefore, a pH of 8.5 was used to label ASF with PLGA NPs. Hydrolysis of the NHS ester, however, is a competing reaction and increases with increasing pH [68]. Hydrolysis occurs more readily in dilute protein or peptide solutions. In concentrated protein solutions, the acylation reaction is favored.
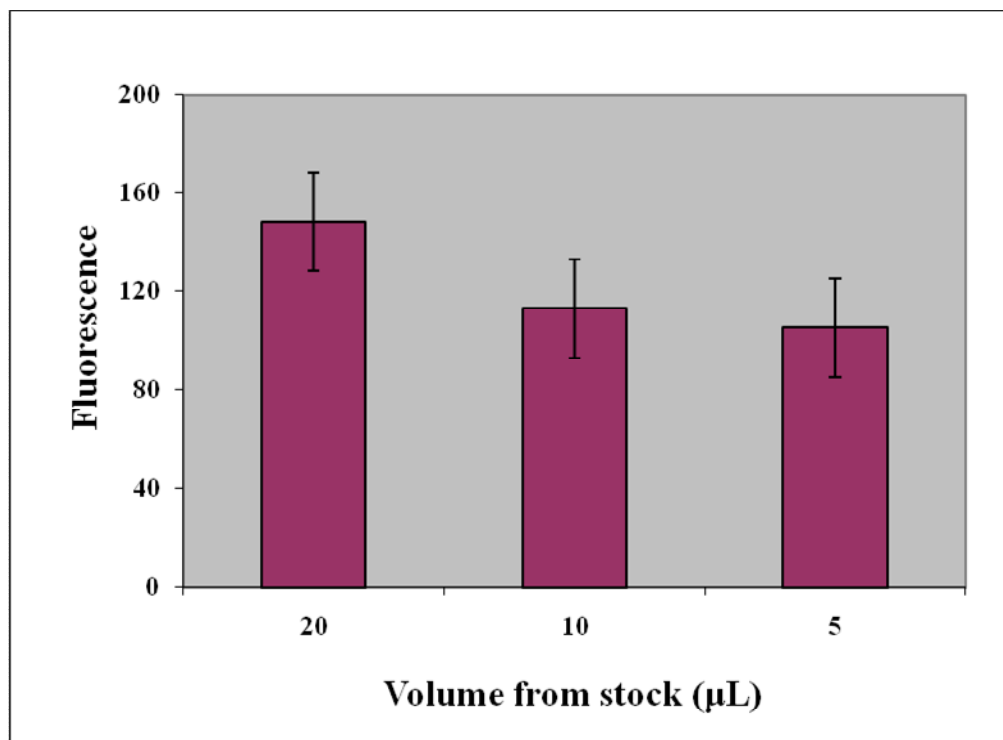
Figure 3.11 Fluorescence intensity of rhodamine labeled ASF as observed using Kodak imager ($\lambda = 575$ nm and $\lambda = 605$ nm).

Dye-protein ratio in the mixture: A ratio of 1:10 dye-protein was used for the conjugation of rhodamine to ASF following the reported procedure [59]. As shown in Figure 3.11, the protein sample showed fluorescence, so at this point it was decided that protein can be used for adsorption on to the PLGA NPs. Dye-protein ratio depends on the concentration of the dye and protein used [70]. Dye-protein conjugate depends on the number of reactive amino groups on the protein. Normally 1:1 or 1:3 dye:protein ratio is used. In the protein labeling kit it is mentioned that over-labeling can cause fluorophore quenching and nonspecific staining. High-labeling may also affect biological/biochemical activity, biodistribution, or clearance of conjugates *in vivo*. Therefore, we decided to work with 1:10 dye-protein ratio and it gave desired results.

Reaction temperature: Labeling is increased by dropping the temperature. It has been revealed that labeling at 4 °C is enhanced compared with that at room temperature by > 35% [70]. Therefore, we carried out the labeling reaction of ASF with rhodamine at 0 °C.

Molecular weight: It has been shown that fluorescence labeling is easier and the intensity of fluorescence is higher for high molecular weight proteins compared to that of low molecular weight proteins [69]. ASF is a large protein with a molecular weight of 48 KDa [35]. This may be why ASF was labeled easily despite of the fact that rhodamine conjugates have a significantly lower quantum yield.

Furthermore, an effect of dissolving rhodamine in different amounts of DMSO was also studied. Rhodamine (1 mg) dissolved in 500 µL, 200 µL or 100 µL DMSO showed labeling, but rhodamine dissolved in less than 100 µL DMSO showed no labeling. Moreover, it was observed that rhodamine dissolved in 500 µL DMSO always gave good amount of labeling, whereas, when dissolved in 100 µL DMSO fluorescence was not observed for small sample volumes (5 µL, Figure 3.11).

3.2.2 Coating Nanoparticle Surface with Asialofetuin

Nanoparticles were incubated overnight with the protein to allow non-specific adsorption onto their surface (step 2, Figure 3.10). The coating was done in phosphate buffer at pH 5 at 4 °C, as it has been shown that pH 5 - 7 yields higher adsorption efficiency [71]. Adsorption of protein onto NPs results from interactions between hydrophobic PLGA polymer and non-polar (hydrophobic) part of the protein [60]. However, hydrophilic protein domains adsorbed better on PLGA NP surfaces prepared using double emulsion than hydrophobic proteins because the outer layer of double emulsion PLGA NP is also hydrophilic. After adsorption, these NPs are washed to remove any unbound protein.

Protein content of NPs was measured using Bradford assay. Absorbance was measured at 595 nm using ELISA reader. A linear plot was obtained for absorbance versus concentration of the standards with R^2 value of 0.966. The concentration of the sample was obtained from the standard curve. It was noticed

that there was very little protein adsorption which was not detectable using Bradford assay.

Protein adsorption was further measured using Lowry assay because Lowry assay is more sensitive than Brandford assay. Absorbance was measured at 550 nm using ELISA reader. A linear plot was obtained for absorbance versus concentration of the standards with R^2 value of 0.999. The concentration of the sample was obtained from the standard curve. However, this method also showed that there was no significant protein adsorption on nanoparticles.

Both methods used to characterize ASF on NP did not show any protein adsorption. This could be because we used small amounts of NPs (0.6 mg), and the protein that could be adsorbed onto NPs was also in small scale. The protein used for adsorption reaction (step 2, Figure 3.10) ranged between 0.2 mg and 0.5 mg. Further, it is possible that lot of NPs were lost during centrifugation. Further, it has been shown that higher physical adsorption of protein to NPs can be seen with ester-terminated PLGA NPs whereas we used COOH terminated PLGA. Higher physical adsorption of protein with ester terminated PLGA may be due to enhanced hydrophobic interaction between PLGA and protein [72].

3.3 Covalent Binding of Asialofetuin (ASF) on PLGA NPs

Chemical conjugation of ASF to NPs was next explored as non-covalent adsorption did not yield sufficient protein on the NPs. The free COOH group of PLGA was used for covalent conjugation of protein to the NPs. ASF and BSA (negative control) were covalently conjugated to PLGA NPs. After successful

70

conjugation, the proteins were covalently labeled with rhodamine as shown in Figure 3.12.
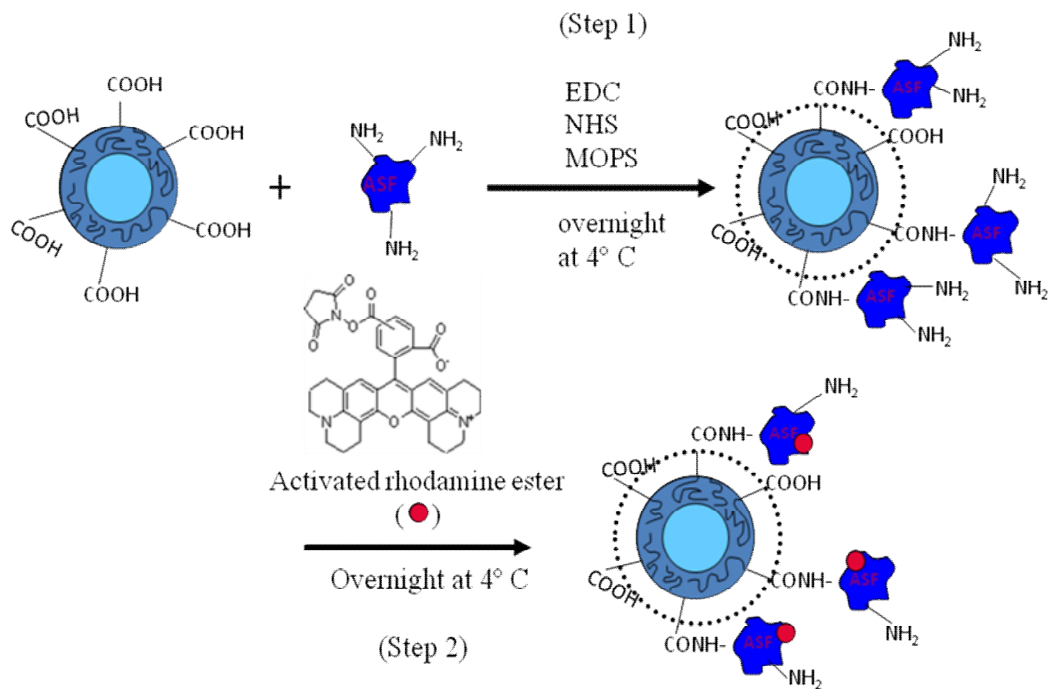
Figure 3.12 Schematic representation of step wise covalent conjugation of ASF on PLGA NPs. (● = rhodamine)

3.3.1 Covalent Conjugation of Asialofetuin to PLGA Nanoparticles

For the covalent modification of PLGA NPs, EDC was reacted with the carboxylic acid group of the PLGA NPs to form an intermediate, o-acylisourea. This intermediate reacts with N-hydroxysuccinimide (NHS) to form an acylamino ester. The activated carboxylate of the PLGA then reacts with free amines from ASF or BSA to form a stable covalently linked conjugate as shown in Figure 3.13 [61]. NPs conjugated with ASF or BSA were characterized by BCA protein assay.

The amount of protein on NP was calculated using the following equation. Protein on NP = amount of incorporation protein (µg) / sample used for the assay (mg).
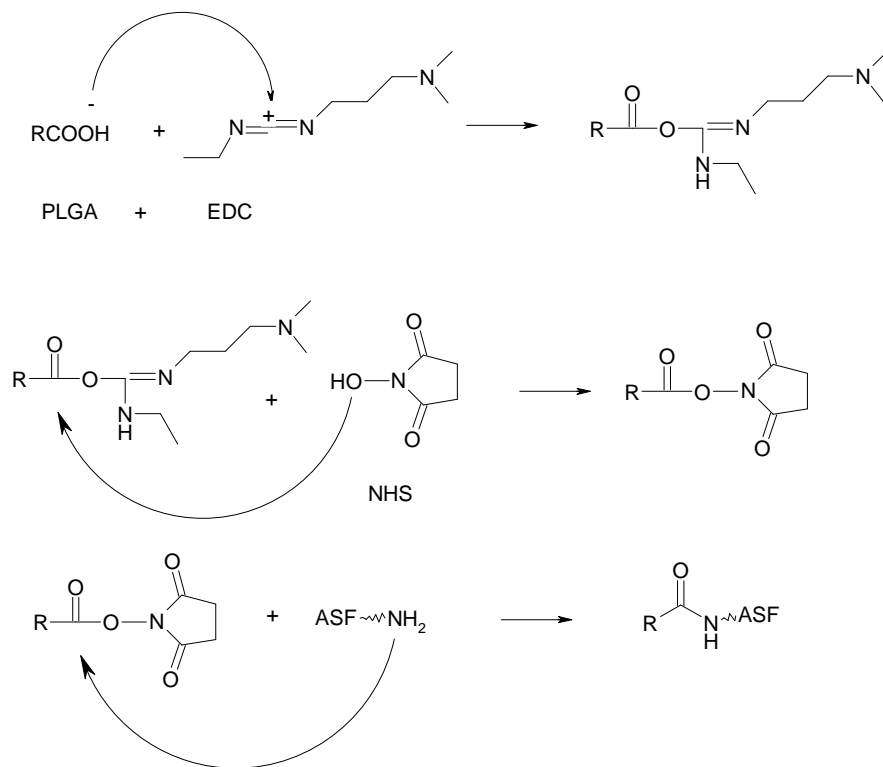
Figure 3.13 Mechanism of covalent conjugation of the protein with PLGA NPs using EDC and NHS as activating agents.

NPs prepared using the ED method and PC or EA as the organic solvents were used for covalent conjugation with ASF protein. NPs prepared using EA as a solvent showed enhanced conjugation with ASF (30.5 µg) and BSA (33.6 µg) compared to PC solvent (13.6 and 1.1 µg) as shown in Table 3.3. Low conjugation using propylene carbonate (PC) solvent could be due to interference from excess PC solvent in the NPs with the protein. PC has activated carboxylate group and it is possible that NH_2 groups from the protein are reacting with PC

solvent resulting in labeling the excess solvent instead COOH groups of NPs. Solvent along with the protein that is attached to the solvent gets removed during centrifugation. The amount of conjugation for ASF and BSA was similar; therefore we used NP-ASF and NP-BSA prepared using EA solvent (in ED method) to study the uptake by hepatocytes.

Table 3.3 Evaluation of asialofetuin loading on PLGA nanoparticles (covalent conjugation) using BCA protein assay.

Nanoparticle	Solvent used during preparation	Protein* ± S.D. (µg)
NP-ASF	PC	13.6 ± 0.39
NP-BSA	PC	1.1 ± 0.23
NP-ASF	EA	30.5 ± 2.50
NP-BSA	EA	33.6 ± 4.50

* Protein (ASF or BSA) present in 1 mg of freeze dried nanoparticle sample. S.D. standard deviation.

3.3.2 Labeling of NP-ASF with Rhodamine

NP-ASF was labeled with rhodamine using the method described by Hermanson G et al. [59]. NP-ASF was labeled with activated NHS-rhodamine ester by stirring the reaction mixture overnight at 4 °C (Figure 3.12). Un-reacted rhodamine was removed by centrifugation. The amount of ASF labeling with rhodamine was measured using Kodak imager. The fluorescence of the samples obtained from the serial dilution of the stock (Table 2.5) was found to decrease with dilution as shown in Figure 3.14. Based on the intensity of control rhodamine (Table 2.5), NP-ASF (20 µL) and NP-BSA (20 µL) contain 0.22 mg and 0.29 mg

rhodamine, respectively. NP-BSA samples showed similar results with a slightly higher fluorescence intensity. ASF and BSA are very similar in size, 40 KDa and 66 KDa, respectively. However ASF is a heavily glycosylated protein and BSA is not. Therefore, BSA may have more NH_2 groups that are available for conjugation leading to enhanced labeling with rhodamine ester.
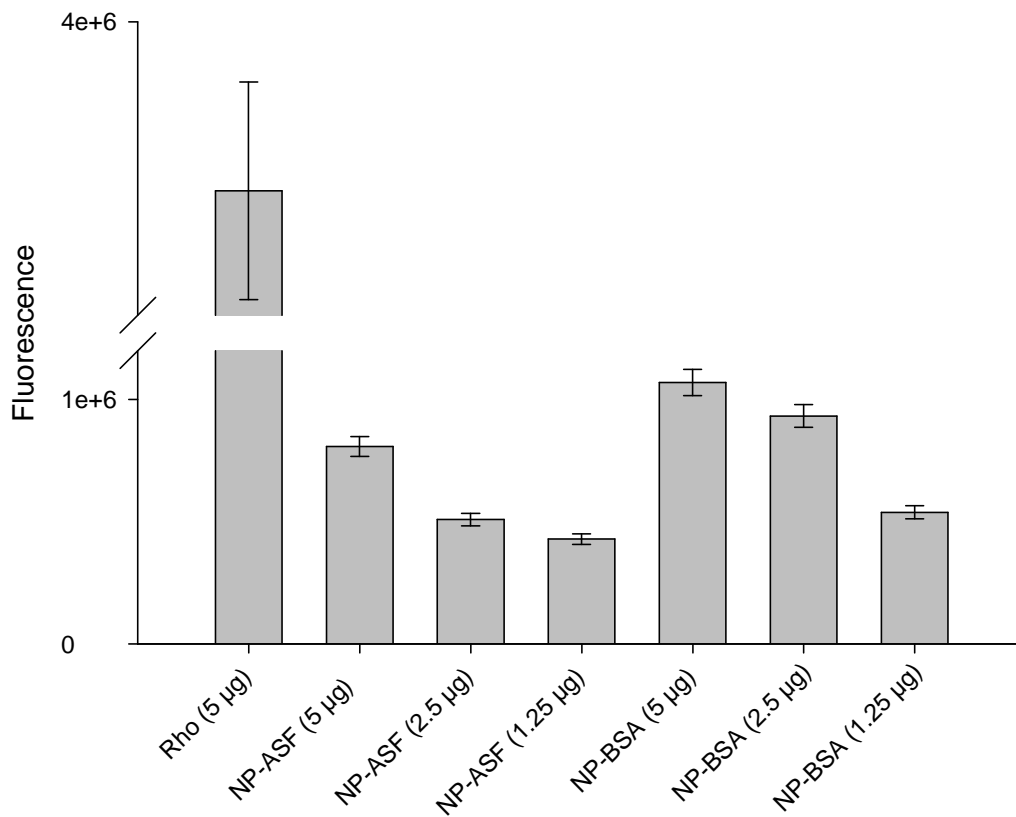
Figure 3.14 Characterization of NP-ASF labeled with rhodamine using Kodak imager. *Excitation = 575 nm and Emission = 605 nm

3.4 Cell-uptake Study

The cell uptake studies of the NP-ASF were done using Hep G2 human liver cancer cell line. The *in vitro* uptake was monitored using fluorescence microscopy and flow cytometry experiments.

3.4.1 NP-ASF Uptake by Hep G2 cells using Fluorescence microscopy

For the microscopy experiment, 10^5 Hep G2 cells were incubated overnight in a 2-well chamber slide with media (3 mL). Following overnight incubation, NP-ASF (0.5 mg or 1 mg) or NP-BSA (0.5 mg or 1 mg) was added to the chamber slide and was incubated for 4 hours. Cells were washed and were observed under the fluorescent microscope.

After incubation with the cells, NP-ASF showed more uptake than NP-BSA as shown in Figure 3.15. NP-ASF and NP-BSA showed some non-specific uptake after 2 hours of incubation (Figure 3.15 a). However, this was mostly eliminated after 4 hours of incubation with NP-ASF and NP-BSA (Figure 3.15 b). Interestingly, after 4 hours of incubation, only one cell showed uptake of NP-BSA but the intensity of the fluorescence was high meaning the amount of NP-BSA uptake by the cell was high (Figure 3.15 b).
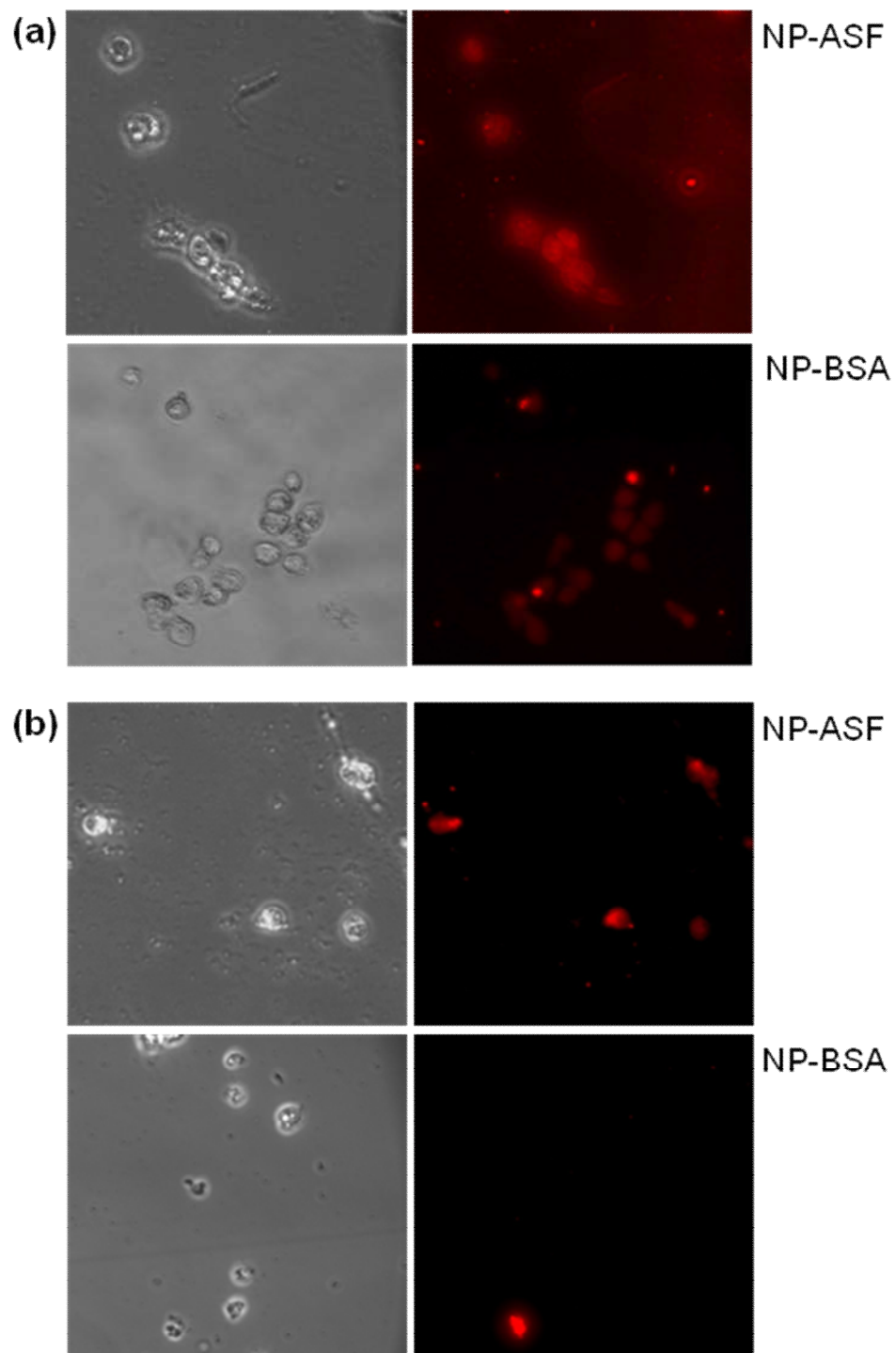
Figure 3.15 Uptake of rhodamine labeled NP-BSA or NP-ASF by Hep G2 cells observed using fluorescent microscope. Left panel shows images taken under translated light and the right panel shows images taken under rhodamine filter. Cells were incubated with NP-BSA or NP-ASF for 2 h (a) or 4 h (b) at 37 ºC.

3.4.2 NP-ASF Uptake by Hep G2 Cells using Flow Cytometry

Flow cytometry was used to compare NP-ASF and NP-BSA uptake by hepatocytes. Hep G2 cells (1 million) were incubated at 37 °C in a 6-well plate with media (3 mL) for 2 hours. NP-ASF (1 mg) or NP-BSA (1 mg) was added to the plate wells and the cells were incubated for overnight. Cells were washed and dissolved in FBS/PBS buffer. Around 500,000 cells were taken for flow cytometry, out of which 10,000 cells were used to analyze the results. The data was analyzed using Dako cytomation summit software. The experiment was done in duplicate.

Figure 3.16 shows the uptake of NP-ASF and NP-BSA by the cells. Vertical axis of the graph obtained from flow cytometry gives us the % gated or the number of cells that have NPs inside them. Horizontal axis shows the fluorescence intensity of the NPs inside the cells. Cells alone showed very little (0.97%) auto fluorescence with a mean fluorescence of 24.8 ± 7.3 (Figure 3.16 a). Cells incubated with NP-BSA (1 mg) showed $61.78 \pm 0.04\%$ of the cells having NPs with a mean fluorescence of 49.2 ± 5.3 (Figure 3.16 b). Whereas, incubation of 1 mg of NP-ASF with cells showed $97.88 \pm 0.01\%$ of the cells having NPs with 56.4 ± 13.2 mean fluorescence as seen in Figure 3.16 c. The results clearly show that ASF conjugation on the surface of NPs greatly enhances the uptake by hepatocytes.

Of note, incubation of the cells with samples at 37 °C is crucial because at low temperature reduced mobility of membrane components can be disadvantageous to bulky ligands with reduced accessibility to binding sites.
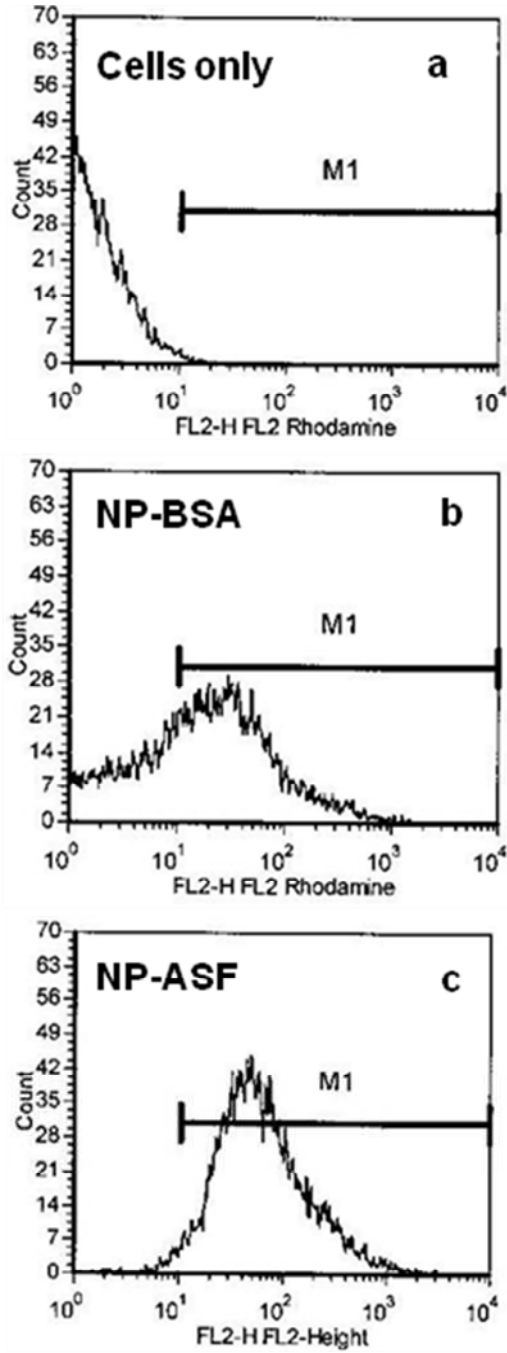
Figure 3.16 Uptake of Rhodamine labeled NP-ASF or NP-BSA by Hep G2 cell line using flow cytometry. (a) Hep G2 cells alone, (b) Hep G2 cells after incubation with NP-BSA, and (c) NP-ASF.

Beyond this, we also studied the uptake of NP-BSA by Hep G2 cells in the presence of increasing amounts of NPs. As the amount of the NPs increases, the uptake also increases. As shown in Figure 3.17, incubation of 0.5 mg, 0.7 mg or 1 mg of NP-BSA showed $19.86 \pm 0.04\%$, $57.86 \pm 0.04\%$ or $61.78 \pm 0.04\%$ uptake by the cells, respectively. The mean fluorescence observed for these three samples was 34.6 ± 13.6, 46.3 ± 4.3 and 49.2 ± 5.3 respectively.
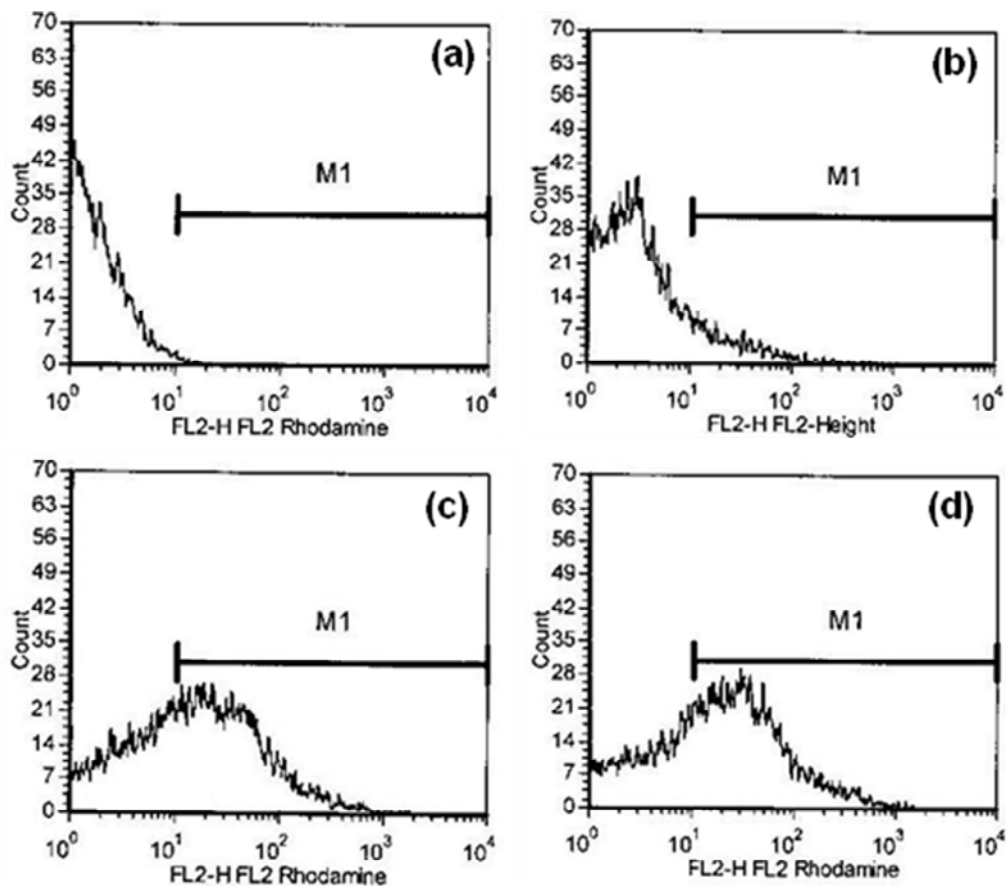

Figure 3.17 Uptake of different amounts of rhodamine labeled NP-BSA by Hep G2 cell line using flow cytometry. (a) Hep G2 cells only, cells incubated with (b) 0.5 mg NP-BSA, (c) 0.7 mg NP-BSA, and (d) 1 mg NP-BSA.

3.4.3 Specific Uptake of NP-ASF by Hep G2 cells via ASF Receptor

In order to check the specificity of NP uptake by ASF receptor, the uptake was studied by blocking the receptor sites. A significant reduction in uptake was observed when cells were incubated with excess ASF followed by addition of NP-ASF. In the presence of ASF, the uptake was around $9.79 \pm 0.03\%$ whereas in the absence of ASF, NP-ASF uptake was around $97.88 \pm 0.01\%$ by the cells (Figure 3.18). The results suggest that the NP-ASF is taken up by the cells via specific receptor mediated mechanism.

Interestingly, it has been shown that if two-thirds of the exposed amino groups of the asialofetuin molecule were modified, the rate of uptake decreased to less than one-fourth [7]. The reduction in endocytic uptake was due to a reduced rate of formation of the receptor ligand complex. Although a number of amino groups of the ASF must be modified in our rhodamine labeled NP-ASF complex, a large number of exposed amino groups must be still available as we observed a significant uptake by the Hep G2 cells. The extent of modification of the protein due to conjugation with PLGA and rhodamine remains to be determined and will help in developing the next generation improved NP-ASF complexes for drug delivery.
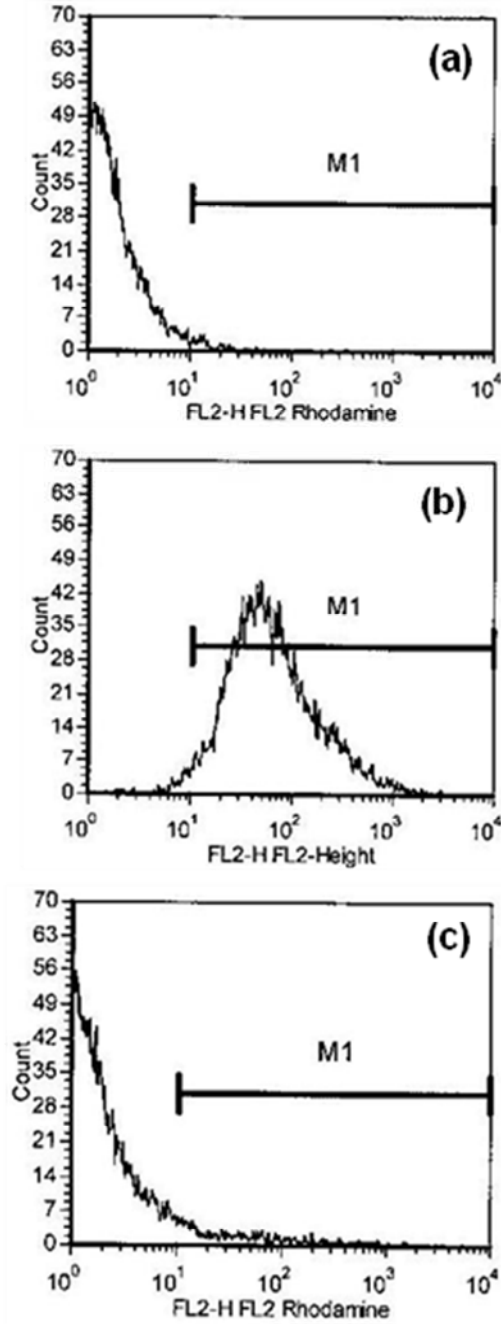
Figure 3.18 FACS analysis for the competitive binding of NP-ASF, showing auto fluorescence of Hep G2 cells (a), fluorescence of cells after incubation with NP-ASF in the absence (b) and presence of ASF (c).

CHAPTER 4. Conclusion and Future Directions

4.1 Concluding Remarks

Current drugs for HCV have many side effects and the dosage is high. Selective targeting of the drug to the liver will result in reduction in side effects, low dosage of the drug taken daily and improvement in efficacy. PLGA NPs were used as a carrier for targeting hepatocytes. Several successful formulations of freeze dried NPs with the size range of 163 - 360 nm using ED method were prepared. Size was measured using Zetasizer. Size and appearance of these NPs was further observed using AFM, which showed that these NPs were spherical. Stability of NPs in solution at 4 °C and -20 °C was evaluated and showed that at 4 °C NPs maintained size for up to 21 days, whereas, at -20 °C there was a size increase within 2 hours.

There are many carbohydrate-specific receptors found on the liver cells specifically hepatocytes. It has been shown that ASF has a high binding capacity to ASGP-R and it greatly increases the uptake during the first four hours. ASF and BSA were coated on to NPs physically and chemically. Physical adsorption did not give the desired results, but ASF and BSA were successfully covalently conjugated to NPs to give NP-ASF and NP-BSA.

Labeling of the protein with fluorescent probes allows us to study the uptake by hepatocytes. Therefore, we covalently conjugated NP-ASF and NP-BSA with rhodamine. Labeling rhodamine to the protein illustrates that increase

in the concentration of rhodamine beyond critical concentration does not result in more labeling. There was, however, a very pronounced effect of pH upon the conjugation efficiency of rhodamine. Temperature at which the reaction is carried at also affects the labeling. It has been shown that better labeling results at lower temperature. Molecular weight is another factor that affects the labeling. High molecular weight proteins tend to show good labeling.

The asialoglycoprotein receptor is known to be present on Hep G2 cells. This receptor is specific for asialoglycoprotein, therefore, we conjugated ASF on the surface of NPs for specific targeting of these NPs to the hepatocytes. PLGA nanoparticles (NP-ASF) bind with the receptor on the surface of the cell membrane and are endocytosed. The uptake of asialofetuin coated NP (NP-ASF) was greater than that of the uptake of BSA coated NP (NP-BSA) by Hep G2 cells. The uptake was studied using fluorescent microscope and flow cytometry. Both techniques gave the same results. Furthermore, it was shown using flow cytometry that the uptake of NP-ASF by hepatocytes was specific. This proves that labeling of NPs with ASF greatly enhances the uptake by hepatocytes. This will result in improvement in efficacy in delivering the drug and will reduce the side effects associated with the current treatment.

4.2 Future Directions

The promising results obtained from specific uptake of ASF conjugated NPs by Hep G2 cells is driving force for us to continue with the project. Our next goal is to encapsulate the drug (ribavirin) inside the PLGA NP carrier and target it to

the hepatocytes. Cohen et al. have reported that addition of Ca^{2+} in the molar ratio of 2:1 of calcium to drug increases the encapsulation of the drug [54]. Ca^{2+} along with ribavirin can be used to increase the encapsulation of ribavirin.

Further a correct method for freeze drying NPs needs to be developed. As mentioned before (Section 3.1.2), aggregation during freeze drying can be prevented by using a correct cryoprotectant or a lyoprotectant. Moreover, an acceptable freeze-dried product can be formed by freezing the formulation at the temperature lower than the collapse temperature (Tc). Such factors can be studied and used to develop a method that can result in elimination of formulation aggregation.

Finally, a peptide could be used to target the NPs to hepatocytes. Wong et al. recently reported a 33-residue peptide derived from P17 protein that targets hepatocytes [73]. P17 is a proximal half of the T7 phage tail fibre protein, found to target recombinant proteins to hepatocytes *in vivo*. It has been shown that targeting signal of p17 was within residues 151 - 267. More recently, the targeting activity has been localized to a peptide of 33 amino acids within the p17 protein. The sequence of the 33-residue peptide is as follows KNESSTNATNTKQWRDETKGFRDEARRFKNTAG. The 33-residue P17 peptide can be used for surface conjugation of PLGA nanoparticles to target hepatocytes.

ASF is a natural large protein therefore it is not easily accessible and is expensive. An ideal drug would have certain features like high affinity and specificity towards its target; manufacturing in large quantities must be relatively

simple; the drug must be highly stable and also soluble at the same time [74]. Successful delivery to the specific target via different routes of administration is important and once it reaches the targeted site it must remain long enough to have the desired therapeutic effect. It has been seen that protein drugs are not extremely successful in achieving most of these attributes. ASF is glycosylated protein which tends to be rapidly cleared and thus will require frequent injection. Given the limitations of protein drug, peptide can be used as an alternative. Peptides have already been used extensively as therapeutics in most of the physiological processes, ranging from neurology, endocrinology and haematology [75]. In contract to proteins, peptides are more stable, inexpensive to produce and convenient in use [76]. The stability of the peptide drug can be increased by putting a beta amino acid or D-amino acid isomers. Beyond this, the modern peptide mimetics theory involves production of small molecules which mimic peptides in order to overcome their ineffectiveness as drugs when administered orally. The small molecules retain the desired biological characteristics of the peptide lead, are stable, have a lot of diversity, and can be designed to provide the new drugs. Therefore it is possible to represent the biologically active sites of the peptides in the form of administered small-molecule mimetics that would have the advantages of evolutionally designed peptides as well as good drug properties.

CHAPTER 5. References

1.   http://www.piercenet.com/Objects/view.cfm?type=Page&ID=412BAC2E-F0BC4ABA-A79B-887E413910AB.

2.   Courant, T.; Roullin, V. G.; Cadiou, C.; Delavoie, F.; Molinari, M.; Andry, M. C.; Chuburu, F., Development and physicochemical characterization of copper complexes-loaded PLGA nanoparticles. *International Journal of Pharmaceutics* **2009,** *379* (2), 226-234.

3.   Longmuir, K. J.; Haynes, S. M.; Baratta, J. L.; Kasabwalla, N.; Robertson, R. T., Liposomal delivery of doxorubicin to hepatocytes in vivo by targeting heparan sulfate. *Int J Pharm* **2009,** *382* (1-2), 222-33.

4.   http://www.elmhurst.edu/~chm/vchembook/558micelle.html.

5.   Vogelson, C. T., Advances in drug delivery systems. *Modern drug discovery* **2001,** *4* (4), 49-52.

6.   Goyal, P.; Goyal, K.; Vijaya Kumar, S. G.; Singh, A.; Katare, O. P.; Mishra, D. N., Liposomal drug delivery systems--clinical applications. *Acta Pharm* **2005,** *55* (1), 1-25.

7.   Roseng, L.; Tolleshaug, H.; Berg, T., Uptake, intracellular transport, and degradation of polyethylene glycol-modified asialofetuin in hepatocytes. *J Biol Chem* **1992,** *267* (32), 22987-93.

8.   Araújo, J.; Vega, E.; Lopes, C.; Egea, M. A.; Garcia, M. L.; Souto, E. B., Effect of polymer viscosity on physicochemical properties and ocular tolerance of FB-loaded PLGA nanospheres. *Colloids and Surfaces B: Biointerfaces* **2009,** *72* (1), 48-56.

9.   Cartiera, M. S.; Johnson, K. M.; Rajendran, V.; Caplan, M. J.; Saltzman, W. M., The uptake and intracellular fate of PLGA nanoparticles in epithelial cells. *Biomaterials* **2009,** *30* (14), 2790-8.

10.   Barichello, J. M.; Morishita, M.; Takayama, K.; Nagai, T., Encapsulation of hydrophilic and lipophilic drugs in PLGA nanoparticles by the nanoprecipitation method. *Drug Dev Ind Pharm* **1999,** *25* (4), 471-6.

11.   Galindo-Rodriguez, S.; Allemann, E.; Fessi, H.; Doelker, E., Physicochemical parameters associated with nanoparticle formation in the salting-

out, emulsification-diffusion, and nanoprecipitation methods. *Pharm Res* **2004,** *21* (8), 1428-39.

12.   Lamprecht, A.; Ubrich, N.; Hombreiro Perez, M.; Lehr, C.; Hoffman, M.; Maincent, P., Biodegradable monodispersed nanoparticles prepared by pressure homogenization-emulsification. *Int J Pharm* **1999,** *184* (1), 97-105.

13.   Csaba, N.; Caamano, P.; Sanchez, A.; Dominguez, F.; Alonso, M. J., PLGA:poloxamer and PLGA:poloxamine blend nanoparticles: new carriers for gene delivery. *Biomacromolecules* **2005,** *6* (1), 271-8.

14.   Packhaeuser, C. B.; Lahnstein, K.; Sitterberg, J.; Schmehl, T.; Gessler, T.; Bakowsky, U.; Seeger, W.; Kissel, T., Stabilization of aerosolizable nano-carriers by freeze-drying. *Pharm Res* **2009,** *26* (1), 129-38.

15.   Kwon, H.-Y.; Lee, J.-Y.; Choi, S.-W.; Jang, Y.; Kim, J.-H., Preparation of PLGA nanoparticles containing estrogen by emulsification-diffusion method. *Colloids and Surfaces A: Physicochemical and Engineering Aspects* **2001,** *182* (1-3), 123-130.

16.   Betancourt, T., Brown, B.; Brannon-Peppas, L.; Poly(Lactide-Co-Glycolide) Nanoparticles for Targeted and Controlled Delivery of Doxorubicin for the Treatment of Cancer. *University of Texas* **2005**.

17.   Mundargi, R. C.; Babu, V. R.; Rangaswamy, V.; Patel, P.; Aminabhavi, T. M., Nano/micro technologies for delivering macromolecular therapeutics using poly(D,L-lactide-co-glycolide) and its derivatives. *J Control Release* **2008,** *125* (3), 193-209.

18.   Tamber, H.; Johansen, P.; Merkle, H. P.; Gander, B., Formulation aspects of biodegradable polymeric microspheres for antigen delivery. *Adv Drug Deliv Rev* **2005,** *57* (3), 357-76.

19.   Miller, R. A.; Brady, J. M.; Cutright, D. E., Degradation rates of oral resorbable implants (polylactates and polyglycolates): Rate modification with changes in PLA/PGA copolymer ratios. *Journal of Biomedical Materials Research* **1977,** *11* (5), 711-719.

20.   J.C.Middleton; Tipton, A. J., *Medical Plastics and Biomaterials* **1998**, 5, 30.

21.   Cai, C.; Mao, S.; Germershaus, O.; Schaper, A.; Rytting, E.; Chen, D.; Kissel, T., Influence of morphology and drug distribution on the release process of FITC-dextran-loaded microspheres prepared with different types of PLGA. *J Microencapsul* **2008**, 1-12.

22.   Prudencio, M.; Rodriguez, A.; Mota, M. M., The silent path to thousands of merozoites: the Plasmodium liver stage. *Nat Rev Micro* **2006,** *4* (11), 849-856.

23.   Ashwell, G.; Harford, J., Carbohydrate-Specific Receptors of the Liver. *Annual Review of Biochemistry* **1982,** *51* (1), 531-554.

24.   Schwartz, A. L.; Rup, D.; Lodish, H. F., Difficulties in the quantification of asialoglycoprotein receptors on the rat hepatocyte. *J Biol Chem* **1980,** *255* (19), 9033-6.

25.   Mandal, D. K.; Brewer, C. F., Cross-linking activity of the 14-kilodalton beta-galactoside-specific vertebrate lectin with asialofetuin: comparison with several galactose-specific plant lectins. *Biochemistry* **1992,** *31* (36), 8465-72.

26.   Pricer, W. E.; Ashwell, G., The Binding of Desialylated Glycoproteins by Plasma Membranes of Rat Liver. *Journal of Biological Chemistry* **1971,** *246* (15), 4825-4833.

27.   Li, Y.; Huang, G.; Diakur, J.; Wiebe, L. I., Targeted delivery of macromolecular drugs: asialoglycoprotein receptor (ASGPR) expression by selected hepatoma cell lines used in antiviral drug development. *Curr Drug Deliv* **2008,** *5* (4), 299-302.

28.   Huang, G.; Diakur, J.; Xu, Z.; Wiebe, L. I., Asialoglycoprotein receptor-targeted superparamagnetic iron oxide nanoparticles. *Int J Pharm* **2008,** *360* (1-2), 197-203.

29.   Schwartz, A. L.; Marshak-Rothstein, A.; Rup, D.; Lodish, H. F., Identification and quantification of the rat hepatocyte asialoglycoprotein receptor. *Proc Natl Acad Sci U S A* **1981,** *78* (6), 3348-52.

30.   Park, J. H.; Cho, E. W.; Shin, S. Y.; Lee, Y. J.; Kim, K. L., Detection of the asialoglycoprotein receptor on cell lines of extrahepatic origin. *Biochem Biophys Res Commun* **1998,** *244* (1), 304-11.

31.   Arangoa, M. A.; Duzgunes, N.; Tros de Ilarduya, C., Increased receptor-mediated gene delivery to the liver by protamine-enhanced-asialofetuin-lipoplexes. *Gene Ther* **2003,** *10* (1), 5-14.

32.   Wu, G. Y.; Wu, C. H., Evidence for targeted gene delivery to Hep G2 hepatoma cells in vitro. *Biochemistry* **1988,** *27* (3), 887-92.

33.   Ponzetto, A.; Fiume, L.; Forzani, B.; Song, S. Y.; Busi, C.; Mattioli, A.; Spinelli, C.; Marinelli, M.; Smedile, A.; Chiaberge, E.; et al., Adenine arabinoside monophosphate and acyclovir monophosphate coupled to lactosaminated albumin

reduce woodchuck hepatitis virus viremia at doses lower than do the unconjugated drugs. *Hepatology* **1991,** *14* (1), 16-24.

34.   Findeis, M. A.; Wu, C. H.; Wu, G. Y., Ligand-based carrier systems for delivery of DNA to hepatocytes. *Methods Enzymol* **1994,** *247*, 341-51.

35.   Wu, J.; Zern, M. A., Modification of liposomes for liver targeting. *J Hepatol* **1996,** *24* (6), 757-63.

36.   Yoshima, H.; Matsumoto, A.; Mizuochi, T.; Kawasaki, T.; Kobata, A., Comparative study of the carbohydrate moieties of rat and human plasma alpha 1-acid glycoproteins. *J Biol Chem* **1981,** *256* (16), 8476-84.

37.   Erion, M. D.; van Poelje, P. D.; MacKenna, D. A.; Colby, T. J.; Montag, A. C.; Fujitaki, J. M.; Linemeyer, D. L.; Bullough, D. A., Liver-Targeted Drug Delivery Using HepDirect Prodrugs. *Journal of Pharmacology and Experimental Therapeutics* **2005,** *312* (2), 554-560.

38.   Palmer, M., *Guide of Hepatitis and Liver Disease.* Penguin Putnam. **2004**, 73-120.

39.   Shepard, C. W.; Finelli, L.; Alter, M. J., Global epidemiology of hepatitis C virus infection. *Lancet Infect Dis* **2005,** *5* (9), 558-67.

40.   Clarke, B., Molecular virology of hepatitis C virus. *J Gen Virol* **1997,** *78*, 2397-410.

41.   Huang, Z.; Murray, M. G.; Secrist, J. A., 3rd, Recent development of therapeutics for chronic HCV infection. *Antiviral Res* **2006,** *71* (2-3), 351-62.

42.   Clément, S.; Pascarella, S.; Negro, F., Hepatitis C Virus Infection: Molecular Pathways to Steatosis, Insulin Resistance and Oxidative Stress. *Viruses* **2009,** *1* (2), 126-143.

43.   Zou, S.; Tepper, M.; El Saadany, S., Prediction of hepatitis C burden in Canada. *Can J Gastroenterol* **2000,** *14* (7), 575-80.

44.   Houghton, M.; Abrignani, S., Prospects for a vaccine against the hepatitis C virus. *Nature* **2005,** *436* (7053), 961-6.

45.   Hsu, H. H.; Abrignani, S.; Houghton, M., Prospects for a hepatitis C virus vaccine. *Clin Liver Dis* **1999,** *3* (4), 901-15.

46.   Brown, R. S., Hepatitis C and liver transplantation. *Nature* **2005,** *436* (7053), 973-8.

47.   http://digestive.niddk.nih.gov/ddiseases/pubs/chronichepc.

48.   Reddy, K. R.; Nelson, D. R.; Zeuzem, S., Ribavirin: current role in the optimal clinical management of chronic hepatitis C. *J Hepatol* **2009,** *50* (2), 402-11.

49.   Wu, J. Z.; Lin, C. C.; Hong, Z., Ribavirin, viramidine and adenosine-deaminase-catalysed drug activation: implication for nucleoside prodrug design. *J Antimicrob Chemother* **2003,** *52* (4), 543-6.

50.   Wu, J.; Nantz, M. H.; Zern, M. A., Targeting hepatocytes for drug and gene delivery: emerging novel approaches and applications. *Front Biosci* **2002,** *7*, 717-25.

51.   Haynes, S. M.; Longmuir, K. J.; Robertson, R. T.; Baratta, J. L.; Waring, A. J., Liposomal polyethyleneglycol and polyethyleneglycol-peptide combinations for active targeting to liver in vivo. *Drug Deliv* **2008,** *15* (4), 207-17.

52.   Lin, A.; Chen, J.; Liu, Y.; Deng, S.; Wu, Z.; Huang, Y.; Ping, Q., Preparation and evaluation of N-caproyl chitosan nanoparticles surface modified with glycyrrhizin for hepatocyte targeting. *Drug Dev Ind Pharm* **2009,** *35* (11), 1348-55.

53.   Wu, J. Z.; Walker, H.; Lau, J. Y.; Hong, Z., Activation and deactivation of a broad-spectrum antiviral drug by a single enzyme: adenosine deaminase catalyzes two consecutive deamination reactions. *Antimicrob Agents Chemother* **2003,** *47* (1), 426-31.

54.   Cohen-Sela, E.; Chorny, M.; Koroukhov, N.; Danenberg, H. D.; Golomb, G., A new double emulsion solvent diffusion technique for encapsulating hydrophilic molecules in PLGA nanoparticles. *J Control Release* **2009,** *133* (2), 90-5.

55.   Choi, S.-W.; Kwon, H.-Y.; Kim, W.-S.; Kim, J.-H., Thermodynamic parameters on poly(,-lactide-co-glycolide) particle size in emulsification-diffusion process. *Colloids and Surfaces A: Physicochemical and Engineering Aspects* **2002,** *201* (1-3), 283-289.

56.   Minsu Lee; Yong Woo Cho; Jae Hyung Park; Hesson Chung; Seo Young Jeong; Kuiwon Choi; Dae Hyuk Moon; Sang Yoon Kim; In-San Kim; Kwon, I. C., Size control of self-assembled nanoparticles by an emulsion/solvent evaporation method *Colloid & Polymer Science* **2006,** *284* (5), 506-512.

57.   Diwan, M.; Elamanchili, P.; Lane, H.; Gainer, A.; Samuel, J., Biodegradable nanoparticle mediated antigen delivery to human cord blood

derived dendritic cells for induction of primary T cell responses. *J Drug Target* **2003,** *11* (8-10), 495-507.

58.   John, S.; Praveen, E.; Manish, D.; Azita, H.; Anahita, D., In *Nanoparticulate Delivery Systems for Control of Immunity*, **2004**, 564-566.

59.   Hermanson, G., *Bioconjugate techniques* **1996**, 322.

60.   Kocbek, P.; Obermajer, N.; Cegnar, M.; Kos, J.; Kristl, J., Targeting cancer cells using PLGA nanoparticles surface modified with monoclonal antibody. *Journal of controlled release* **2007,** *120* (1-2), 18-26.

61.   Kalkanidis, M.; Pietersz, G. A.; Xiang, S. D.; Mottram, P. L.; Crimeen-Irwin, B.; Ardipradja, K.; Plebanski, M., Methods for nano-particle based vaccine formulation and evaluation of their immunogenicity. *Methods* **2006,** *40* (1), 20-9.

62.   Banker, G.; Rhodes, C., *Modern pharmaceutics* 4th ed.; New york, **2002**, 121, 261-271.

63.   Chorny, M.; Fishbein, I.; Danenberg, H. D.; Golomb, G., Lipophilic drug loaded nanospheres prepared by nanoprecipitation: effect of formulation variables on size, drug recovery and release kinetics. *J Control Release* **2002,** *83* (3), 389-400.

64.   Sahana, D. K.; Mittal, G.; Bhardwaj, V.; Kumar, M. N., PLGA nanoparticles for oral delivery of hydrophobic drugs: influence of organic solvent on nanoparticle formation and release behavior in vitro and in vivo using estradiol as a model drug. *J Pharm Sci* **2008,** *97* (4), 1530-42.

65.   Jeon, H. J.; Jeong, Y. I.; Jang, M. K.; Park, Y. H.; Nah, J. W., Effect of solvent on the preparation of surfactant-free poly(DL-lactide-co-glycolide) nanoparticles and norfloxacin release characteristics. *Int J Pharm* **2000,** *207* (1-2), 99-108.

66.   Banga, A. K., *Therapeutic Peptides and Proteins: Formulation, Processing, and Delivery Systems* 2nd ed.; Taylor & Francis Group: **2006**, 354.

67.   Tang, X.; Pikal, M. J., Design of freeze-drying processes for pharmaceuticals: practical advice. *Pharm Res* **2004,** *21* (2), 191-200.

68.   http://www.piercenet.com/files/2080as4.pdf.

69.   Shan, Y.; Wang, L.; Shi, Y.; Zhang, H.; Li, H.; Liu, H.; Yang, B.; Li, T.; Fang, X.; Li, W., NHS-mediated QDs-peptide/protein conjugation and its application for cell labeling. *Talanta* **2008,** *75* (4), 1008-14.

70.   Taki, M.; Shiota, M.; Taira, K., Transglutaminase-mediated N- and C-terminal fluorescein labeling of a protein can support the native activity of the modified protein. *Protein Engineering, Design and Selection* **2004,** *17* (2), 119-126.

71.   Chesko, J.; Kazzaz, J.; Ugozzoli, M.; O'Hagan D, T.; Singh, M., An investigation of the factors controlling the adsorption of protein antigens to anionic PLG microparticles. *J Pharm Sci* **2005,** *94* (11), 2510-9.

72.   Nelson, R. D.; Shibata, N.; Podzorski, R. P.; Herron, M. J., Candida mannan: chemistry, suppression of cell-mediated immunity, and possible mechanisms of action. *Clin. Microbiol. Rev.* **1991,** *4* (1), 1-19.

73.   Wong, S. C.; Wakefield, D.; Klein, J.; Monahan, S. D.; Rozema, D. B.; Lewis, D. L.; Higgs, L.; Ludtke, J.; Sokoloff, A. V.; Wolff, J. A., Hepatocyte Targeting of Nucleic Acid Complexes and Liposomes by a T7 Phage p17 Peptide. *Molecular Pharmaceutics* **2006,** *3* (4), 386-397.

74.   Tomlinson, I. M., Next-generation protein drugs. *Nat Biotechnol* **2004,** *22* (5), 521-2.

75.   Edwards, C. M. B.; Cohen, M. A.; Bloom, S. R., Peptides as drugs. *Q J Med* **1999,** *92*, 1-4.

76.   www.peptideguide.com.

APPENDEX
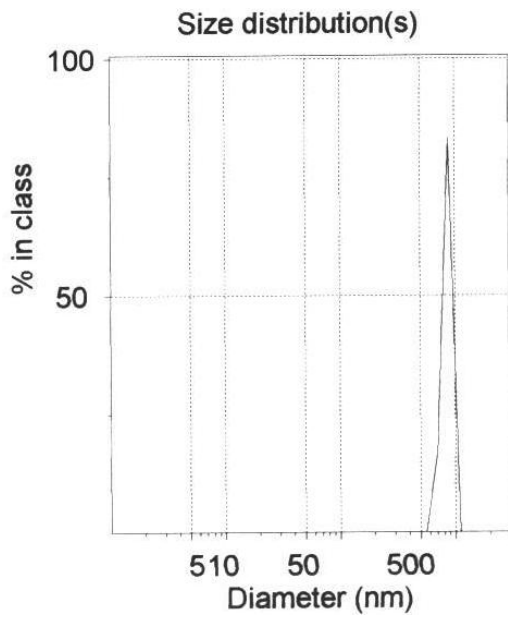
Figure A1 The size distribution of PLGA NPs prepared using DESE method with respect to variation 1 (Figure 3.4).
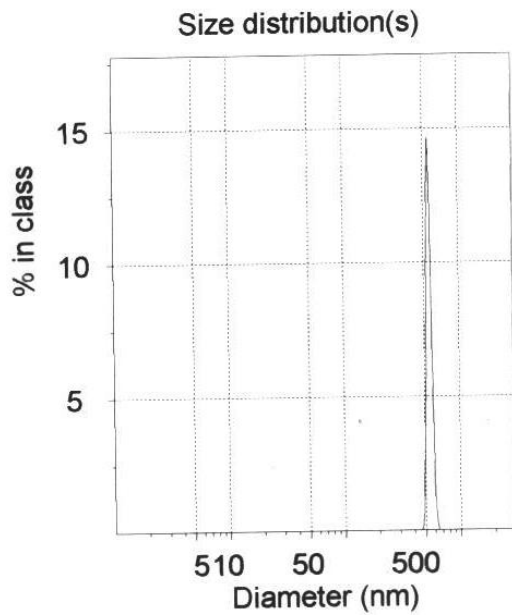

Figure A2 The size distribution of PLGA NPs prepared using DESE method with respect to variation 2 (Figure 3.4).
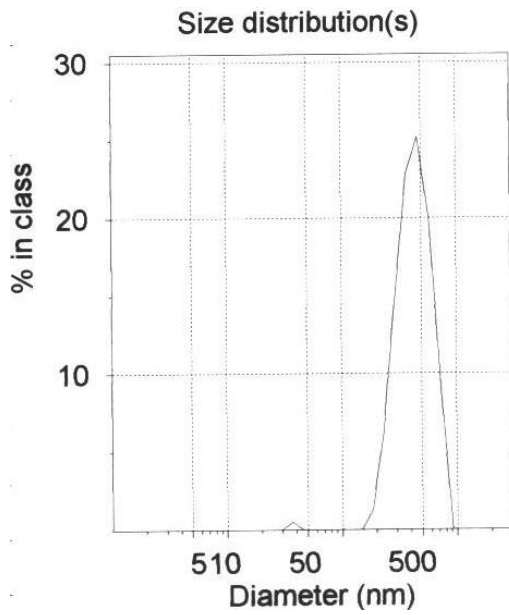
Figure A3 The size distribution of PLGA NPs prepared using DESE method with respect to variation 3 (Figure 3.4).
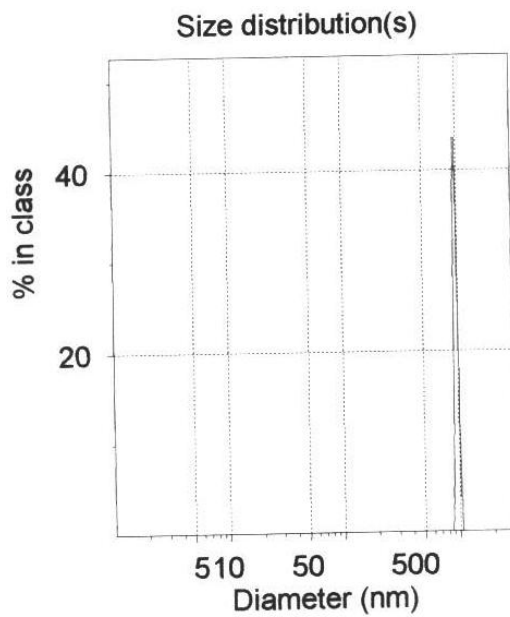

Figure A4 The size distribution of PLGA NPs prepared using DESE method with respect to variation 4 (Figure 3.4).
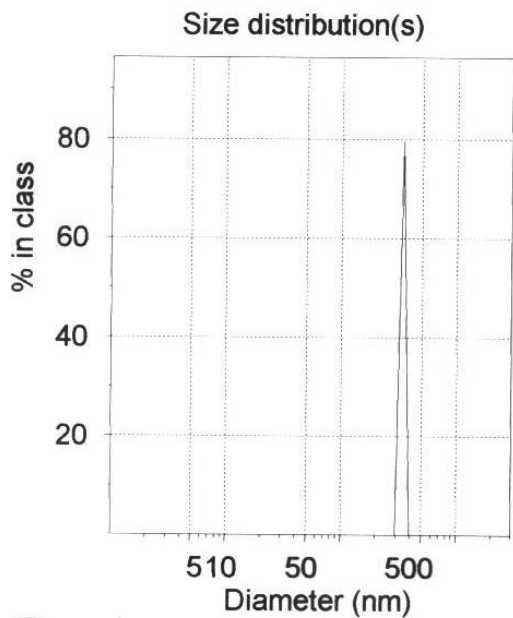
Figure A5 The size distribution of PLGA NPs prepared using DESE method with respect to variation 5 (Figure 3.4).
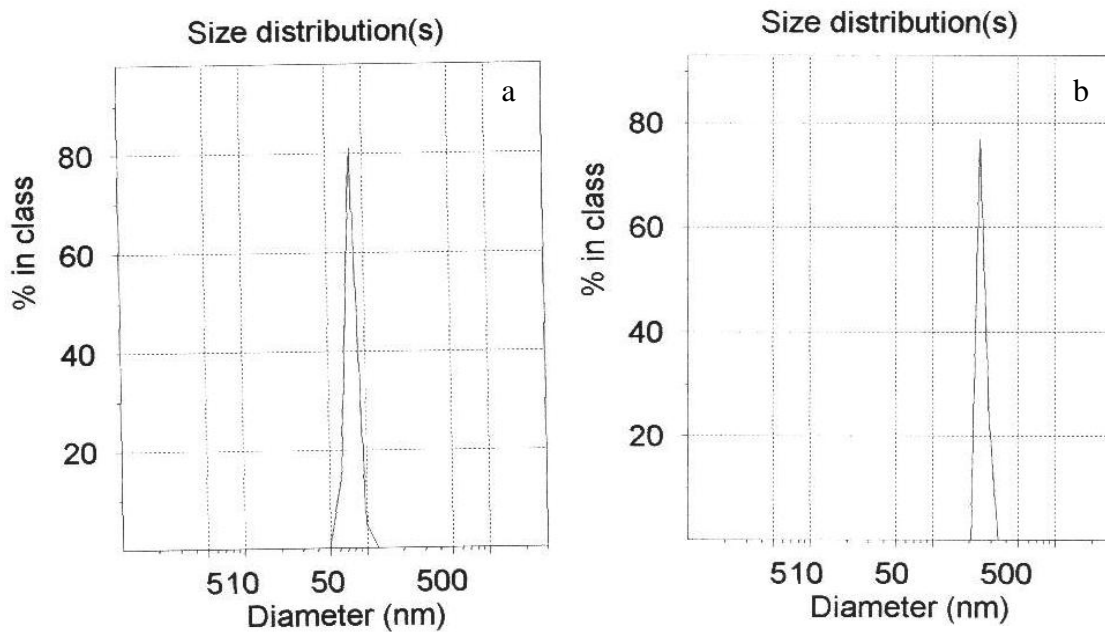

Figure A6 Size distribution of PLGA NPs, using Zetasizer, before freeze drying (a) and after freeze drying (b) prepared using EA as a solvent in ED method.